Trajectory planning for unmanned surface vehicles in multi-ship encounter situations

Jianjian Liu [a,b], Huizi Chen [a], Shaorong Xie [a], Yan Peng [a], Dan Zhang [a,*], Huayan Pu [a]

[a] *School of Mechatronic Engineering and Automation, Shanghai University, Shanghai, 200444, China*
[b] *Shanghai Artificial Intelligence Laboratory, Shanghai, 200232, China*

ARTICLE INFO

ABSTRACT

Unmanned surface vehicles (USVs) can encounter traffic ships while navigating toward the target location. For the USVs, collision avoidance (CA) trajectories need to be planned according to the international regulations for preventing collisions at sea (COLREGS). A novel trajectory planning approach is proposed for the collision-free trajectories planning of USVs in the case of multiship encounters. Unlike the existing trajectory planning approaches, the proposed approach uses the holistic thinking to simplify the analysis of encounter situations. Ships approaching from all sides of the USV are treated as one or two equivalent obstacles based on consistent offset velocity direction (COVD) method. Furthermore, planned velocity is designed using the proposed CA strategy and kinematic constraints. This strategy is compliant with COLREGS and includes an emergency CA module to further ensure a safe distance between the USV and traffic ships. The performance of the proposed trajectory planning approach is verified through physical simulations using an existing simulator. The simulation results show that the proposed trajectory planning approach can implement multiple USVs to simultaneously avoid collisions and reach their respective target positions. Moreover, the approach remains effective when other USVs do not follow the COLREGS protocols.

1. Introduction

Unmanned surface vehicles (USVs), which are highly autonomous ships, are a reliable means of improving the efficiency of water for applications such as scientific exploration, safety patrols, emergency search and rescue, and hydrographic surveys. USVs can encounter traffic-ships while navigating toward the target location. To ensure safe navigation, USVs must plan collision avoidance (CA) trajectories according to international regulations for preventing collisions at sea (COLREGS) (International Maritime Organization, 1972).

Various algorithms have been used to address trajectory planning limitations, such as fuzzy logic (Hwang et al., 2001), A* (Loe, 2008), ant colony optimization (Tsou and Hsueh, 2010), Dijkstra (Medyna and Mąka, 2012), Voronoi diagram (Candeloro et al., 2013), velocity obstacle (VO) (Fiorini and Shiller, 1998; Junmin et al., 2021), artificial potential field (APF) (Wu et al., 2015; Lyu and Yin, 2019), fast marching method (Liu et al., 2015), deep reinforcement learning (Cheng and Zhang, 2018), rapidly-exploring random tree (RRT*) (Zaccone and Martelli, 2020), and model predictive control (Sun et al., 2022), among others. However, most trajectory planning algorithms are designed with

only static obstacles or a single dynamic obstacle in mind or do not incorporate COLREGS. To some extent, this limits the scope of their practical applications at sea.

With the rapid development of ship autonomy and the increasing complexity of maritime traffic, the trajectory planning problem in multiship encounters has attracted the attention of many scholars, and many research outcomes have been proposed to date. A probabilistic obstacle processing method based on radar sensor information for target tracking considers the measurement and tracking uncertainties and uses a grid-based path search algorithm to generate avoidance trajectories (Blaich et al., 2015). To search for the optimal global trajectory at a low replanning frequency, a fully coupled deliberative planner based on an improved RRT* algorithm was proposed (Yang et al., 2019). Global deliberative planning uses a multistep look-ahead search to compute a global optimal trajectory. Other alternatives include graph-based methods such as A* and its variants (LaValle, 2006). The main challenge that these methods pose is computational efficiency when avoiding collisions. As the dimensionality of the state space and the complexity of the environment increase, the computation time increases significantly. As a reactive method, the VO method is fast because it does

---

not involve complex coupling. CA is achieved by mapping obstacles into the velocity space to form cone-shaped obstacle regions, and selecting the appropriate planning velocity outside these regions (Fiorini and Shiller, 1998). This method was implemented considering COLREGS and was demonstrated in water (Kuwata et al., 2013). Several variants have been derived from VO, including the generalized VO (Huang et al., 2019), probabilistic VO (Kluge and Prassler, 2004), reciprocal VO (Van den Berg et al., 2008), hybrid reciprocal VO (Snape et al., 2011), and dynamic reciprocal VO method (Kufoalor et al., 2018). It is worth noting that the COLREGS provides only fundamental guidelines without detailed quantitative criteria. Therefore, in some encounter situations, two USVs may experience conflict because of incongruous evasive actions taken (Zhang et al., 2015; Woerner et al., 2016). To solve this problem, a symmetric role classification criterion based on COLREGS was proposed, and the probabilistic VO method was applied (Cho et al., 2020).

However, some existing trajectory planning approaches consider only the ideal encounter situation of traffic ships navigating at a constant velocity. In the real world, both manually operated and automated vessels generally adopt CA maneuvers when they encounter collision hazards. To make collision-free trajectory planning methods practical, it is necessary to assume that traffic ships have a certain level of intelligence. It is also necessary to consider unexpected cases in which these ships cannot implement CA measures owing to mechanical failures. In addition, existing COLREGS-compliant CA approaches extensively use relative bearing and relative course to analyze encounter situations, and thus assign stand-on or give-way responsibilities to encountering ships. When multiple ships approach a USV from different directions simultaneously, the encounter situations can become extremely complex and vary. It is difficult to plan safe and effective CA maneuvers for USVs using these approaches. Indeed, traditional VO and APF methods do not effectively handle such complex encounter situations when considering COLREGS. The computational cost of the algorithm increases significantly with the complexity of the encounter situations. Thus, in particularly complex encounters, the USV cannot avoid collisions. In summary, it is highly challenging for a USV to implement COLREGS-compliant trajectory planning considering the realistic situations, particularly when surrounded by multiple ships simultaneously.

In this study, a novel approach was proposed to solve the trajectory planning problem of USVs in multiship encounters. It is assumed that the USVs navigate toward their respective target positions with or without the proposed trajectory planning approach. Each USV treats the other USVs as obstacles. Based on sensor data, a USV performs collision risk assessment for each detected obstacle. If there is no collision risk during navigation, the USV tracks at the desired velocity. Otherwise, the USV enters the CA procedure and plans a collision-free trajectory in real time according to the dynamic environment. In the proposed CA approach, the designed CA velocity is obtained by adding an offset velocity to the desired velocity of the USV, such that the USV can approach the target position while avoiding obstacles. The consistent offset velocity direction (COVD) method is used to determine a suitable offset velocity direction such that the USV has sufficient safe maneuvering space to avoid all collision-hazardous obstacles simultaneously. To simplify the analysis of encounter situations, an equivalent obstacle method is proposed to project all collision-hazardous obstacles in the offset velocity direction. Furthermore, these obstacles are simplified to one or two equivalent obstacles, and the encounter situations were classified into three cases. Moreover, a COLREGS-compliant CA strategy was proposed based on these three encounter situations. The strategy includes an emergency CA module to ensure that a safe distance is maintained between the USV and the obstacles.

This paper has the following main contributions:

1) A novel reactive trajectory planning method was proposed for USVs in multiship encounters. USVs require sufficient space for safe maneuvering to avoid all collision-hazardous obstacles approaching simultaneously from different directions. In this approach, the COVD method is used to determine the appropriate offset velocity direction. All collision-hazardous obstacles are projected onto the offset velocity direction to facilitate the design of a suitable offset velocity in a multi-obstacle environment. Thus, the two-dimensional collision-free trajectory planning problem is simplified into a one-dimensional collision-free offset velocity planning problem.

2) In the proposed CA procedure, the equivalent obstacle concept is innovatively presented to simplify the analysis of the encounter situations. The encounter situations are classified into three cases using the proposed equivalent obstacle method.

3) A COLREGS-compliant CA strategy is proposed based on the above three encounter situations. This strategy is effective regardless of whether the encountered ships obey COLREGS.

Section 2 describes the proposed trajectory planning approach. The proposed CA procedure is described in Section 3. Section 4 presents the physical simulations results for the verification of the proposed algorithm. Finally, conclusions are presented in Section 5. This paper presents the units according to the System International (SI) standards of measurement unless otherwise specified.

2. Trajectory planning in dynamic environment

Influenced by the marine environment and trafficking ships, USVs require real-time trajectory planning to safely reach their target positions. A flowchart of the proposed trajectory planning approach is shown in Fig. 1. First, the desired velocity of the USV in its current state is designed according to the target position. Subsequently, a collision risk assessment is performed for the detected obstacles based on the sensor data. Obstacles with a collision risk with the USV are marked as activated, whereas others are deactivated. When at least one activated obstacle is present, the USV enters the proposed CA procedure and determines the CA velocity. The CA procedure is described in detail in
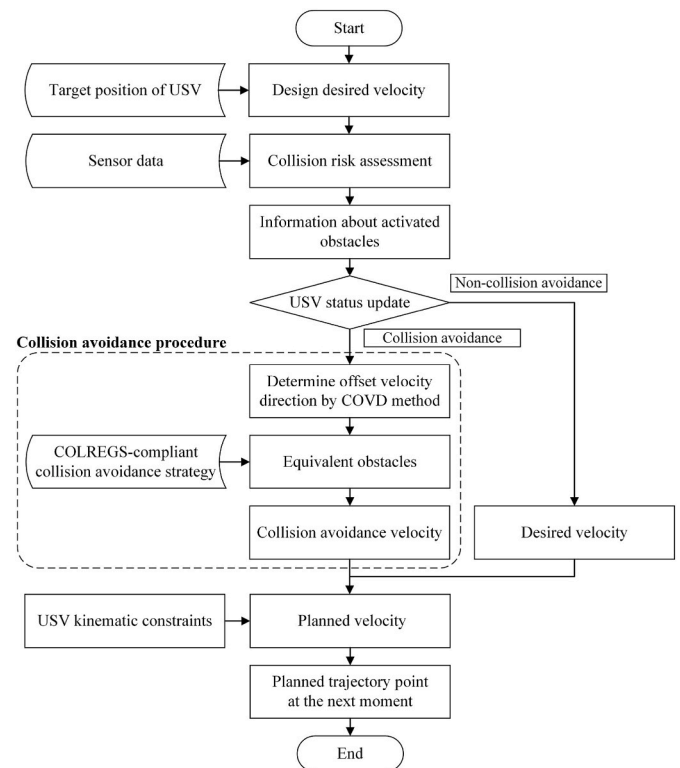

Fig. 1. Flowchart of proposed trajectory planning approach: The dashed box is the CA procedure.

Section 3. Finally, the planned velocity satisfying the USV kinematic constraints is designed based on the CA velocity or the desired velocity, and the planned trajectory point at the next moment is obtained.

2.1. Design of desired velocity

Assuming that the target position and the current motion information of the USV are available, constant-bearing (CB) guidance was used for the USV to move to the target position (Breivik, 2010). The desired velocity of the USV can be obtained as

$$\vec{v}_d = U_d \frac{\vec{p}_t - \vec{p}}{\left\| \vec{p}_t - \vec{p} \right\|} \tag{1}$$

where $\vec{p}_t$ and $\vec{p}$ denote the target and current USV positions, respectively. U_d denotes the desired approach speed toward the target position. $\| \bullet \|$ represents the vector modulus.

$$U_d = \begin{cases} U_{dmax}, & k_p \left\| \vec{p}_t - \vec{p} \right\| > U_{dmax} \\ k_p \left\| \vec{p}_t - \vec{p} \right\|, & others \end{cases} \tag{2}$$

where U_{dmax} denotes the maximum approach speed toward the target position. $k_p > 0$ affects the deceleration behavior of the USV when it reaches the target position.

2.2. Collision risk assessment

The proposed collision risk assessment algorithm was performed in the velocity space using velocity obstacles. Based on the sensor data, obstacles detected by the USV in real time were classified as activated or deactivated to facilitate the CA procedure. Obstacles with a collision risk with the USV are marked as activated, whereas others are considered deactivated.

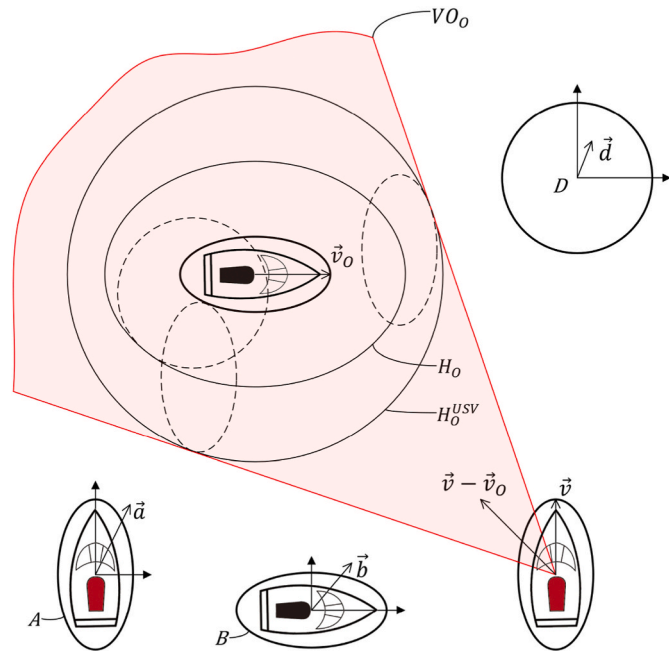To facilitate the calculation of the VO, we treated the USV as a point and expanded the obstacles (Kuwata et al., 2013). Fig. 2 shows a USV of shape A moving with velocity $\vec{v}$, and $A = \{\vec{a} \mid \vec{a} \in A\}$; similarly, an obstacle of shape B is considered as moving with velocity $\vec{v}_o$, and $B = \{\vec{b} \mid \vec{b} \in B\}$. The safe distance between the USV and obstacle boundaries is defined as d_s. D is a circle with radius d_s and $D = \{\vec{d} \mid \vec{d} \in D\}$. And VO is expressed by the following set operations:

Minkowski sum:

$$A \oplus B = \left\{ \vec{a} + \vec{b} \mid \vec{a} \in A, \vec{b} \in B \right\} \tag{3}$$

reflection:

$$-A = \{ -\vec{a} \mid \vec{a} \in A \} \tag{4}$$

When the USV is treated as a point, the hazardous area of the obstacle relative to the USV is

$$H_O^{USV} = B \oplus D \oplus -A \tag{5}$$

The VO formed by the obstacle in the velocity space of the USV relative to the obstacle is then given by

$$VO_O = \left\{ \vec{v} - \vec{v}_O \mid \lambda\left(\vec{p}, \vec{v} - \vec{v}_o\right) \cap \left(H_O^{USV} + \vec{p}_O\right) \neq \varnothing \right\} \tag{6}$$

where $\vec{p}_O$ denotes the position vector of the obstacle. $\lambda(\vec{p}, \vec{v} - \vec{v}_o)$ denotes the ray starting from position $\vec{p}$ in the direction of $\vec{v} - \vec{v}_o$.

The desired relative velocity $\vec{v}_d^O$ and actual relative velocity $\vec{v}^O$ of the USV relative to the obstacle are expressed as follows:

$$\begin{cases} \vec{v}_d^O = \vec{v}_d - \vec{v}_o \\ \vec{v}^O = \vec{v} - \vec{v}_o \end{cases} \tag{7}$$

When $\vec{v}_d^O \in VO_O$, USV inevitably collides with the expanded obstacle in the process of approaching target position with velocity $\vec{v}_d$. t_d denotes the time to collision of the USV with an expanded obstacle. In addition, when $\vec{v}^O \in VO_O$, the USV may collide with an expanded obstacle in the near future. t_a denotes the time to collision of the USV with an expanded

Fig. 2. VO formed by the obstacle relative to USV: When $\vec{v} - \vec{v}_o$ is outside the VO_O, there is no collision risk between USV and the obstacle. $H_O = B \oplus D$. $H_O^{USV} = B \oplus D \oplus -A$. VOs mentioned later are processed by obstacle expansion.
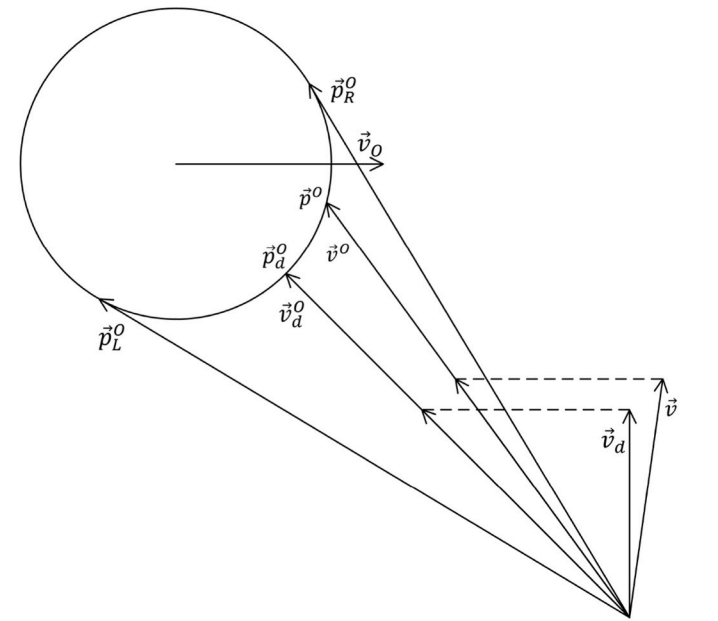

Fig. 3. Collision risk assessment: The circle represents the expanded obstacle. $\vec{p}_L^O$ and $\vec{p}_R^O$ denote the position vectors from USV to left tangent point and right tangent point of expanded obstacle, respectively.

obstacle. As shown in Fig. 3, t_d and t_a are expressed as

$$
\begin{cases}
t_d = \left\| \overrightarrow{p}_d^O \right\| / \left\| \overrightarrow{v}_d^O \right\| \\
t_a = \| \overrightarrow{p}^O \| / \| \overrightarrow{v}^O \|
\end{cases}
\tag{8}
$$

where $\overrightarrow{p}_d^O$ is the position vector from the current position of the USV along velocity $\overrightarrow{v}_d^O$ to the boundary of the expanded obstacle. And $\overrightarrow{p}^O$ is the position vector from the current position of the USV along the velocity $\overrightarrow{v}^O$ to the boundary of the expanded obstacle. Extremely large t_d and t_0 indicate that a long time exists before the USV collides with an obstacle. At this time, it is not necessary for the USV to implement the CA measures. Therefore, the CA reaction time t_r can be used as a threshold to determine the risk of collision in the short term.

In summary, an obstacle is marked as activated if the following conditions are satisfied:

$$
\begin{cases}
\overrightarrow{v}_d^O \in VO_O \\
t_d \le t_r
\end{cases}
or
\begin{cases}
\overrightarrow{v}^O \in VO_O \\
t_a \le t_r
\end{cases}
\tag{9}
$$

2.3. Kinematic constraints

According to the current status of the USV, its desired planned velocity is given by

$$
\overrightarrow{v}_{p0} =
\begin{cases}
\overrightarrow{v}_c, & \text{Collision avoidance} \\
\overrightarrow{v}_d, & \text{Non-collision avoidance}
\end{cases}
\tag{10}
$$

where $\overrightarrow{v}_c$ denotes the CA velocity obtained using the CA procedure described in Section 3. Although the current velocity $\overrightarrow{v}$ of the USV cannot be switched to $\overrightarrow{v}_{p0}$ immediately, it can gradually converge to the $\overrightarrow{v}_{p0}$ through course angle and speed controls. However, the USV motion trajectory may get perturbed if $\overrightarrow{v}_{p0}$ is frequently outside the maneuverable range of the USV.

To make the planned trajectory of USV practical and smooth, the following constraints are input to the planned course angle Ψ_p and planned speed V_p.

$$
\begin{cases}
\Psi_p \in [R\Psi_{min}, R\Psi_{max}] \\
V_p \in [RV_{min}, RV_{max}]
\end{cases}
\tag{11}
$$

where $R\Psi_{min}$ and $R\Psi_{max}$ are the currently reachable minimum and maximum course angles, respectively, relative to the current course angle Ψ. RV_{min} and RV_{max} are the currently reachable minimum and maximum translational speeds relative to the current translational speed V, and are defined as follows:

$$
\begin{cases}
R\Psi_{min} = \Psi + W_{min} t_\Delta \\
R\Psi_{max} = \Psi + W_{max} t_\Delta \\
RV_{min} = V + a_{Vmin} t_\Delta \\
RV_{max} = V + a_{Vmax} t_\Delta
\end{cases}
\tag{12}
$$

where W_{min} and W_{max} denote the minimum and maximum rotational speeds, respectively. a_{Vmin} and a_{Vmax} are the minimum and maximum translational accelerations, respectively. t_Δ is the time interval.

Therefore, the designed planned course angle and speed are expressed as:

$$
\Psi_p =
\begin{cases}
\angle \overrightarrow{v}_{p0}, & \angle \overrightarrow{v}_{p0} \in [R\Psi_{min}, R\Psi_{max}] \\
R\Psi_{min}, & \left(\angle \overrightarrow{v}_{p0} - R\Psi_{min} \right) \backslash 2\pi > \pi, \\
R\Psi_{max}, & \text{others}
\end{cases}
\tag{13}
$$

$$
V_p =
\begin{cases}
\left\| \overrightarrow{v}_{p0} \right\|, & \left\| \overrightarrow{v}_{p0} \right\| \in [RV_{min}, RV_{max}] \\
RV_{min}, & \left\| \overrightarrow{v}_{p0} \right\| < RV_{min} \\
RV_{max}, & \text{others}
\end{cases}
\tag{14}
$$

where $\angle \bullet \in [0, 2\pi)$ denotes the plane angle between the vector and due north (clockwise is positive). The symbol '\' indicates the operation of taking the remainder. The planned velocity is expressed as follows:

$$
\overrightarrow{v}_p = \left(V_p \cos \Psi_p, V_p \sin \Psi_p \right).
\tag{15}
$$

Further, the planned trajectory point at the next moment is

$$
\overrightarrow{p}_p = \overrightarrow{p} + \overrightarrow{v}_p t_\Delta . \#
\tag{16}
$$

In summary, when m obstacles are detected, the trajectory planning process is implemented as shown in Algorithm 1.

Algorithm 1. Trajectory Planning

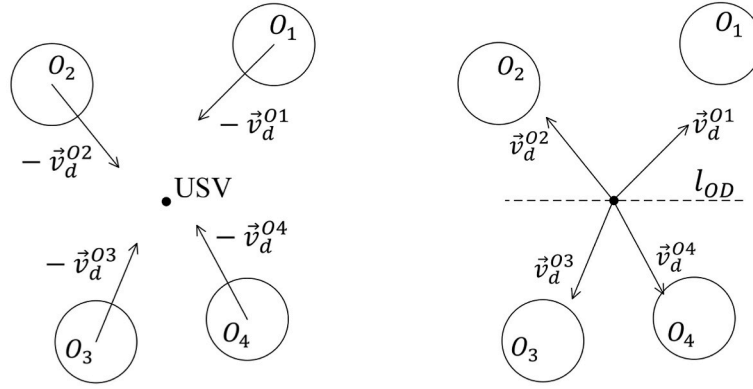| **Algorithm 1** Trajectory Planning |
|---|
| **Input:** t_r, U_d, $\vec{p}_t$, $\vec{v}$, $\vec{p}$, each obstacle $\{VO_O, \vec{v}_O, \vec{p}_O\}$ |
| **Output:** $\vec{v}_p$, $\vec{p}_p$ |
| **Procedure:** |
| 1: compute $\vec{v}_d$ according to (1)-(2) |
| 2: **if** $m = 0$ **then** |
| 3: $\vec{v}_{p0} \leftarrow \vec{v}_d$ |
| 4: **else** |
| 5:   **for** $i = 1$ **to** m **do** |
| 6:   determine if the obstacle is activated by (3)-(9) |
| 7:   **end for** |
| 8:   **if** none of the detected obstacles are activated **then** |
| 9: $\vec{v}_{p0} \leftarrow \vec{v}_d$ |
| 10:   **else** |
| 11:   enter proposed CA procedure and compute $\vec{v}_c$ |
| 12: $\vec{v}_{p0} \leftarrow \vec{v}_c$ |
| 13:   **end if** |
| 14: **end if** |
| 15: compute $\vec{v}_p$ according to (11)-(15) |
| 16: compute $\vec{p}_p$ according to (16) |

3. Collision avoidance procedure

This section describes the proposed CA approach in detail. The CA procedure only requires the consideration of activated obstacles. In general, the designed CA velocity is obtained by adding an offset velocity to the desired velocity of the USV, such that the USV can approach the target position while avoiding obstacles.

We assumed that the number of activated obstacles is n and n is a non-negative integer. O_i represents the i-th activated obstacle, where $i \ne 0$ and $i = 1, 2, ..., n$. $\overrightarrow{v}_d^{Oi}$ represents the desired relative velocity of the USV with respect to the activated obstacle O_i. l_{OD} represents a straight line parallel to the offset velocity.

3.1. COVD method

As shown in Fig. 4(a), when a USV moving with $\overrightarrow{v}_d$ is used as a reference, activated obstacles approach from all directions around USV with $-\overrightarrow{v}_d$. In other words, if the USV moves with $\overrightarrow{v}_d$, it simultaneously approaches each activated obstacle at different velocities, as shown in Fig. 4(b). For a single obstacle O_i, the USV can avoid obstacle O_i more efficiently when the angle between l_{OD} and $\overrightarrow{v}_d^{Oi}$ is the largest (i.e., $l_{OD} \perp \overrightarrow{v}_d^{Oi}$). For multiple obstacles, the USV must find a suitable offset velocity direction such that it has sufficient space for safe maneuver and

(a) Activated obstacles approach from all directions around USV with $-\vec{v}_d^{Oi}$

(b) USV approach each activated obstacle with different velocities at the same time

Fig. 4. USV encounters multiple activated obstacles: l_{OD} represents the straight line parallel to the offset velocity.

avoids all activated obstacles simultaneously. Therefore, the angle (minimum angle) between l_{OD} and all $\vec{v}_d^{Oi}$ should be as large as possible.

θ represents the set of angles formed between adjacent vectors in the set V_d^O.

$$V_d^O = \left\{ \vec{v}_d^{O1}, \vec{v}_d^{O2}, \ldots, \vec{v}_d^{On}, -\vec{v}_d^{O1}, -\vec{v}_d^{O2}, \ldots, -\vec{v}_d^{On} \right\} \tag{17}$$
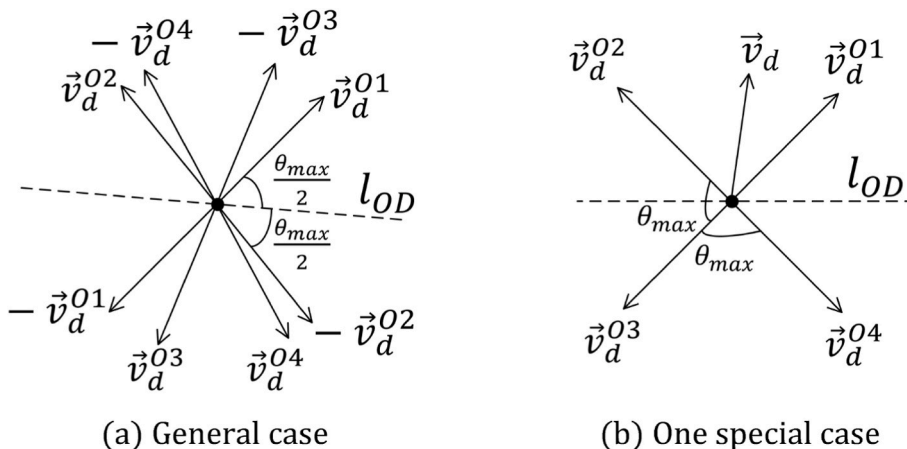
$$\theta = \{\theta_1, \theta_2, \ldots, \theta_{2n}\} \tag{18}$$

The line l_i bisects θ_i. The line l_{max} bisects θ_{max}, where θ_{max} is the maximum value in the set θ. In a general case, as shown in Fig. 5(a), we can design $l_{OD} = l_{max}$. However, in certain special cases, as shown in Fig. 5(b), more than one l_{max} value corresponds to θ_{max}. Owing to the physical features of the USV dynamics, it is easier to change the course angle than to change the speed. Steering is prioritized over acceleration and deceleration to facilitate the CA maneuver of USV. Therefore, the following cost function was designed to select a suitable l_{OD}.

$$J_{OD}(l_i) = \theta_i + w\beta_i, \tag{19}$$

where w is the weight. β_i is the angle between l_i and $\vec{v}_d$. The l_{OD} obtained using these parameters is expressed as

$$l_{OD} = \arg\max_{l_i} J_{OD}(l_i) \tag{20}$$

3.2. Equivalent obstacle method

In general, a USV must analyze the encounter scenario to perform appropriate CA maneuvers. The encounter scenario becomes extremely complex when multiple activated obstacles approach the USV from different directions. In this study, we used holistic thinking to simplify the analysis of encounter situations. In other words, the activated obstacles approaching from all sides of the USV were treated as one or two equivalent obstacles, according to the offset velocity direction.

We assumed that multiple activated obstacles simultaneously approached the USV from different directions, as shown in Fig. 6. The coordinate axis OD was established in the positive direction, in the same direction as $\overrightarrow{OD}$. $\overrightarrow{OD}$ represents the unit vector parallel to l_{OD} and its direction points to the right of $\vec{v}_d$. The obstacles can be divided into two parts with l_{OD} as the boundary: forward and rear obstacles. Obstacles satisfying the following conditions were marked as forward obstacles and others were considered as rear obstacles.

$$\left(\angle \vec{v}_d^{Oi} - \angle \overrightarrow{OD} \right) \backslash 2\pi \in [\pi, 2\pi]. \tag{21}$$

The category of O_i is denoted by D_{Oi}.

$$D_{Oi} = \begin{cases} 1, & \text{forward obstacle} \\ -1, & \text{rear obstacle} \end{cases} \tag{22}$$

First, we analyzed the case of a USV avoiding a single forward obstacle. To facilitate the determination of the offset velocity of the USV

(a) General case

(b) One special case

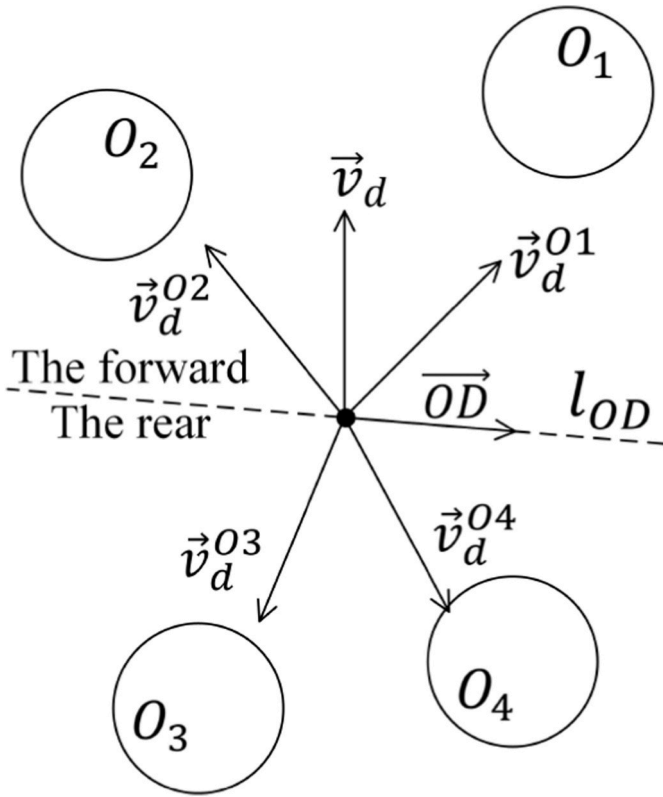**Fig. 5.** Determination of the direction of offset velocity.

Fig. 6. Activated obstacles are divided into two parts: forward and rear obstacles.

during CA, we projected O_i onto the OD axis, as shown in Fig. 7(a). $\overrightarrow{v}_{ODL}^{Oi}$ and $\overrightarrow{v}_{ODR}^{Oi}$ are the critical offset velocities and can be obtained from the following conditions:

$$\begin{cases} \overrightarrow{v}_{ODL}^{Oi} \parallel \overrightarrow{OD} \\ \overrightarrow{v}_{d}^{Oi} + \overrightarrow{v}_{ODL}^{Oi} \parallel \overrightarrow{p}_{L}^{Oi} \end{cases} and \begin{cases} \overrightarrow{v}_{ODR}^{Oi} \parallel \overrightarrow{OD} \\ \overrightarrow{v}_{d}^{Oi} + \overrightarrow{v}_{ODR}^{Oi} \parallel \overrightarrow{p}_{R}^{Oi} \end{cases}, \tag{23}$$

where the symbol '$\parallel$' indicates parallel. The projections of $\overrightarrow{v}_{ODL}^{Oi}$ and $\overrightarrow{v}_{ODR}^{Oi}$ on the OD axis are expressed as:

$$OD_{ODL}^{Oi} = \overrightarrow{v}_{ODL}^{Oi} \cdot \overrightarrow{OD}, \tag{24}$$

$$OD_{ODR}^{Oi} = \overrightarrow{v}_{ODR}^{Oi} \cdot \overrightarrow{OD}. \tag{25}$$

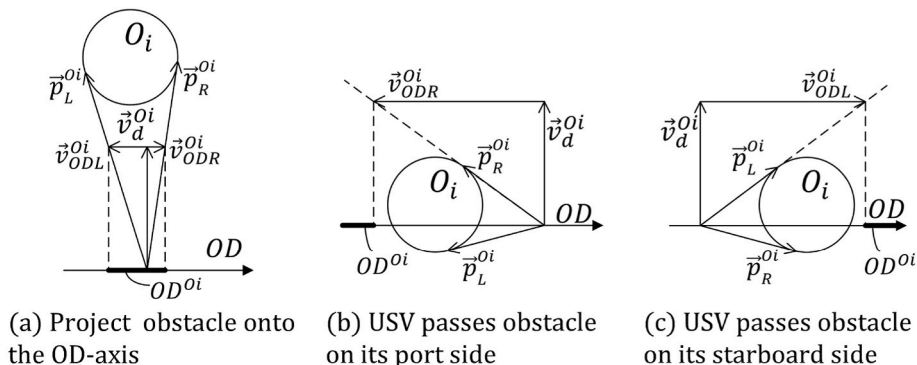Therefore, the projection of O_i onto the OD axis can be expressed as

the value range OD^{Oi}. The choice of the offset velocity should avoid $OD^{Oi} \cdot \overrightarrow{OD}$.

$$OD^{Oi} = \left\{ od^{Oi} \mid od^{Oi} \in \left(OD_{min}^{Oi}, OD_{max}^{Oi} \right) \right\}, \tag{26}$$

where OD_{min}^{Oi} and OD_{max}^{Oi} denote the minimum and maximum values in the range OD^{Oi}. These are expressed as

$$\begin{cases} OD_{min}^{Oi} = \min \left(OD_{ODL}^{Oi}, OD_{ODR}^{Oi} \right) \\ OD_{max}^{Oi} = \max \left(OD_{ODL}^{Oi}, OD_{ODR}^{Oi} \right) \end{cases}. \tag{27}$$

1) If the USV turns toward the starboard to pass O_i on its port side, the OD^{Oi} gradually moves to the left and expands as the USV approaches O_i. Moreover, as shown in Fig. 7(b), the value of OD_{ODL}^{Oi} becomes infinitesimal when the following conditions are satisfied.

$$\begin{cases} D_{Oi} = 1 \\ \left(\angle \left(\overrightarrow{p}_{Oi} - \overrightarrow{p} \right) - \angle \overrightarrow{v}_{d}^{Oi} \right) \Big\backslash 2\pi \in [\pi, 2\pi] \\ \left(\angle \overrightarrow{p}_{L}^{Oi} - \angle \overrightarrow{OD} \right) \Big\backslash 2\pi \in [0, \pi] \end{cases}, \tag{28}$$

where $\overrightarrow{p}_{Oi}$ and $\overrightarrow{p}$ denote the current positions of O_i and the USV, respectively. Further, OD_{ODR}^{Oi} becomes infinitesimal when the following conditions are satisfied:

$$\begin{cases} D_{Oi} = 1 \\ \left(\angle \left(\overrightarrow{p}_{Oi} - \overrightarrow{p} \right) - \angle \overrightarrow{v}_{d}^{Oi} \right) \Big\backslash 2\pi \in [\pi, 2\pi] \\ \left(\angle \overrightarrow{p}_{R}^{Oi} - \angle \overrightarrow{OD} \right) \Big\backslash 2\pi \in [0, \pi] \end{cases}. \tag{29}$$

2) If the USV turns to the port to pass O_i on its starboard side, the OD^{Oi} gradually moves right and expands as the USV approaches O_i. As shown in Fig. 7(c), OD_{ODL}^{Oi} and OD_{ODR}^{Oi} become infinite when conditions (30) and (31) are satisfied.

$$\begin{cases} D_{Oi} = 1 \\ \left(\angle \left(\overrightarrow{p}_{Oi} - \overrightarrow{p} \right) - \angle \overrightarrow{v}_{d}^{Oi} \right) \Big\backslash 2\pi \in [0, \pi] \\ \left(\angle \overrightarrow{p}_{L}^{Oi} - \angle \overrightarrow{OD} \right) \Big\backslash 2\pi \in [0, \pi] \end{cases}, \tag{30}$$

(a) Project obstacle onto the OD-axis

(b) USV passes obstacle on its port side

(c) USV passes obstacle on its starboard side

Fig. 7. USV avoids single forward obstacle.

$$\begin{cases} D_{Oi} = 1 \\ \left(\angle\left(\overrightarrow{p}_{Oi} - \overrightarrow{p}\right) - \angle\overrightarrow{v}_d^{Oi}\right) \Big\backslash 2\pi \in [0, \pi] \\ \left(\angle\overrightarrow{p}_R^{Oi} - \angle\overrightarrow{OD}\right) \Big\backslash 2\pi \in [0, \pi] \end{cases}. \tag{31}$$

Therefore, (24) and (25) can be transformed to

$$OD_{ODL}^{Oi} = \begin{cases} -\infty, & \text{(28) is satisfied} \\ +\infty, & \text{(30) is satisfied} \\ \overrightarrow{v}_{ODL}^{Oi} \cdot \overrightarrow{OD}, & \text{others} \end{cases} \tag{32}$$

$$OD_{ODR}^{Oi} = \begin{cases} -\infty, & \text{(29) is satisfied} \\ +\infty, & \text{(31) is satisfied} \\ \overrightarrow{v}_{ODR}^{Oi} \cdot \overrightarrow{OD}, & \text{others} \end{cases} \tag{33}$$

We then analyzed the case of a USV that avoids a single rear obstacle. As previously mentioned, we projected O_i onto the OD axis, as shown in Fig. 8(a).

1) If the USV turns toward the starboard to pass O_i on its port side, the OD^{Oi} gradually moves to the left and expands as the USV approaches O_i. As shown in Fig. 8(b), OD_{ODL}^{Oi} and OD_{ODR}^{Oi} become infinitesimal when conditions (34) and (35) are satisfied.

$$\begin{cases} D_{Oi} = -1 \\ \left(\angle\left(\overrightarrow{p}_{Oi} - \overrightarrow{p}\right) - \angle\overrightarrow{v}_d^{Oi}\right) \Big\backslash 2\pi \in [0, \pi] \\ \left(\angle\overrightarrow{p}_L^{Oi} - \angle\overrightarrow{OD}\right) \Big\backslash 2\pi \in [\pi, 2\pi] \end{cases} \tag{34}$$

$$\begin{cases} D_{Oi} = -1 \\ \left(\angle\left(\overrightarrow{p}_{Oi} - \overrightarrow{p}\right) - \angle\overrightarrow{v}_d^{Oi}\right) \Big\backslash 2\pi \in [0, \pi] \\ \left(\angle\overrightarrow{p}_R^{Oi} - \angle\overrightarrow{OD}\right) \Big\backslash 2\pi \in [\pi, 2\pi] \end{cases}. \tag{35}$$

2) If the USV turns to the port to pass O_i on its starboard side, the OD^{Oi} gradually moves to the right and expands as the USV approaches O_i. As shown in Fig. 8(c), OD_{ODL}^{Oi} and OD_{ODR}^{Oi} become infinite when conditions (36) and (37) are satisfied.

$$\begin{cases} D_{Oi} = -1 \\ \left(\angle\left(\overrightarrow{p}_{Oi} - \overrightarrow{p}\right) - \angle\overrightarrow{v}_d^{Oi}\right) \Big\backslash 2\pi \in [\pi, 2\pi] \\ \left(\angle\overrightarrow{p}_L^{Oi} - \angle\overrightarrow{OD}\right) \Big\backslash 2\pi \in [\pi, 2\pi] \end{cases} \tag{36}$$

$$\begin{cases} D_{Oi} = -1 \\ \left(\angle\left(\overrightarrow{p}_{Oi} - \overrightarrow{p}\right) - \angle\overrightarrow{v}_d^{Oi}\right) \Big\backslash 2\pi \in [\pi, 2\pi] \\ \left(\angle\overrightarrow{p}_R^{Oi} - \angle\overrightarrow{OD}\right) \Big\backslash 2\pi \in [\pi, 2\pi] \end{cases}. \tag{37}$$

In summary, for a single activated obstacle O_i approaching the USV from any direction, its projection on the OD axis can be solved using (26) and (27). Here, OD_{ODL}^{Oi} and OD_{ODR}^{Oi} can be expressed as

$$OD_{ODL}^{Oi} = \begin{cases} -\infty, & \text{(28) or (34) is satisfied} \\ +\infty, & \text{(30) or (36) is satisfied} \\ \overrightarrow{v}_{ODL}^{Oi} \cdot \overrightarrow{OD}, & \text{others} \end{cases} \tag{38}$$

$$OD_{ODR}^{Oi} = \begin{cases} -\infty, & \text{(29) or (35) is satisfied} \\ +\infty, & \text{(31) or (37) is satisfied} \\ \overrightarrow{v}_{ODR}^{Oi} \cdot \overrightarrow{OD}, & \text{others} \end{cases}. \tag{39}$$

Finally, we analyzed the case of a USV encountering multiple activated obstacles simultaneously. Existing COLREGS-compliant CA methods extensively use relative bearing and relative course to analyze encounter situations and thus assign give-way or stand-on responsibilities to USV. When there are multiple obstacles to the approaching USV from different directions, there can be various encounter situations. These methods can become highly complex when analyzing encounter situations.
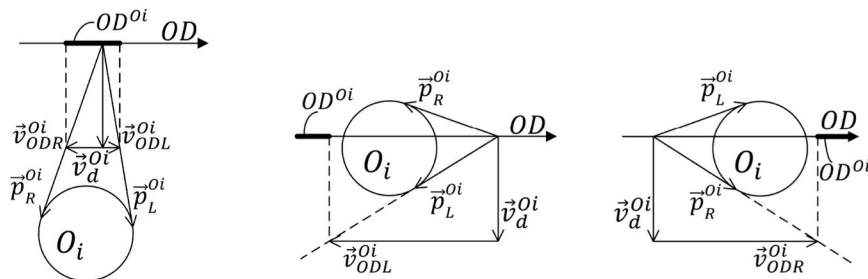
To simplify the analysis of the encounter situations, all forward obstacles were projected onto the OD axis and simplified to the forward-equivalent obstacle EO^f, as shown in Fig. 9(a). Similarly, all the rear obstacles were projected onto the OD axis and simplified to the rear-equivalent obstacle EO^r, as shown in Fig. 9(b).

$$\begin{cases} EO^f = \left\{eo^f \mid eo^f \in \left(EO_{min}^f, EO_{max}^f\right)\right\} \\ EO^r = \left\{eo^r \mid eo^r \in \left(EO_{min}^r, EO_{max}^r\right)\right\} \end{cases}, \tag{40}$$

where EO_{min}^f and EO_{max}^f denote the minimum and maximum EO^f values, and EO_{min}^r and EO_{max}^r denote the minimum and maximum values of EO^r. They are expressed as

(a) Project obstacle onto the OD-axis

(b) USV passes obstacle on its port side

(c) USV passes obstacle on its starboard side

Fig. 8. USV avoids single rear obstacle.

(a) Forward equivalent obstacle EO^f (b) Rear equivalent obstacle EO^r
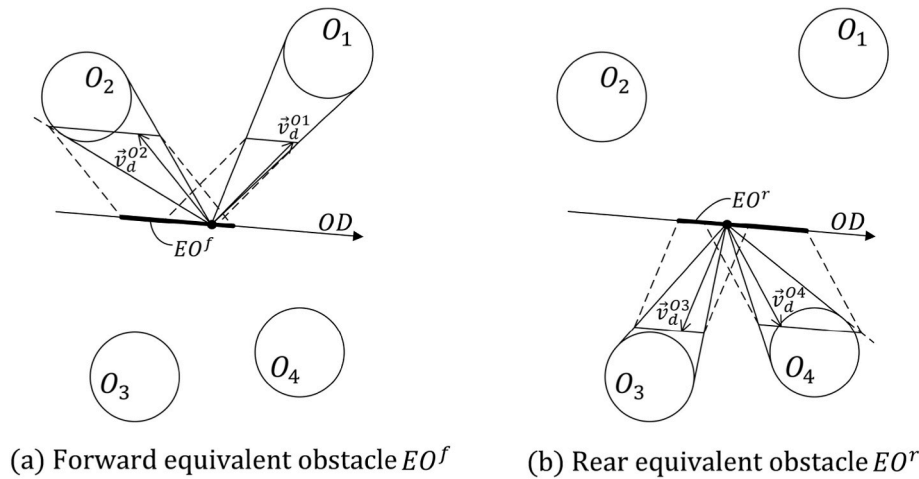
Fig. 9. Equivalent obstacles: (a) all forward obstacles are projected onto OD axis and simplified to forward equivalent obstacle EO^f. (b) all rear obstacles are projected onto OD-axis and simplified to rear equivalent obstacle EO^r.

$$\begin{cases} EO_{min}^f = \min \left(\bigcup_{i=1}^n OD^{fOi} \right) \\ EO_{max}^f = \max \left(\bigcup_{i=1}^n OD^{fOi} \right) \end{cases}, \tag{41}$$

$$\begin{cases} EO_{min}^r = \min \left(\bigcup_{i=1}^n OD^{rOi} \right) \\ EO_{max}^r = \max \left(\bigcup_{i=1}^n OD^{rOi} \right) \end{cases}, \tag{42}$$

where OD^{fOi} and OD^{rOi} denote the projections of the forward and rear obstacles on the OD axis, respectively. These are expressed as follows:

$$OD^{fOi} = \begin{cases} OD^{Oi}, & D_{Oi} = 1 \wedge OD_{min}^{Oi} \neq OD_{max}^{Oi} \\ \varnothing, & others \end{cases} \tag{43}$$

$$OD^{rOi} = \begin{cases} OD^{Oi}, & D_{Oi} = -1 \wedge OD_{min}^{Oi} \neq OD_{max}^{Oi} \\ \varnothing, & others \end{cases} \tag{44}$$

In summary, there are three encounter situations for the USV in the proposed CA procedure.

1) Encounter situation $S = 1$.

When $\forall i = 1, \ldots, n, D_{Oi} = 1$, the USV must avoid the forward-equivalent obstacle EO^f only, that is, the choice of offset velocity $\vec{v}_{OD}$ should satisfy

$$\vec{v}_{OD} \cdot \overrightarrow{OD} \notin EO^f \tag{45}$$

2) Encounter situation $S = -1$.

When $\forall i = 1, \ldots, n, D_{Oi} = -1$, the USV must avoid the rear equivalent obstacle EO^r only, that is, the choice of offset velocity $\vec{v}_{OD}$ should satisfy

$$\vec{v}_{OD} \cdot \overrightarrow{OD} \notin EO^r \tag{46}$$

3) Encounter situation $S = 0$.

When $\exists i, j = 1, \ldots, n \wedge D_{Oi} = 1 \wedge D_{Oj} = -1$, the USV must avoid both the forward equivalent obstacle EO^f and the rear equivalent obstacle

EO^r, that is, the choice of offset velocity $\vec{v}_{OD}$ should satisfy

$$\vec{v}_{OD} \cdot \overrightarrow{OD} \notin EO^f \cup EO^r \tag{47}$$

3.3. COLREGS-compliant collision avoidance strategy

COLREGS 13–17 state a set of compliant actions that a ship can take in three ship encounter situations: head-on, crossing, and overtaking. Despite such regulations, implementing the simultaneous collision avoidance of multiple USVs may not be simple because COLREGS provides only fundamental guidelines without detailed quantitative criteria. To facilitate evasive USV actions in multi-USV encounter situations, the following assumptions were made in this study based on COLREGS 13–17:

1) According to COLREGS 14, when a USV approaches an obstacle head-on, it turns toward the starboard to pass through the obstacle on its port side, as shown in Fig. 10(a).
2) According to COLREGS 15, when a USV crosses from the port side of an obstacle, it turns toward the starboard to pass through the obstacle on its port side, as shown in Fig. 10(b).
3) According to COLREGS 15–17, when a USV crosses the starboard side of an obstacle, it should stand on or turn toward the starboard to pass the obstacle on its port side. Considering that obstacles responsible for giving way may not comply with COLREGS or evade too late, the USV takes CA measures for all activated obstacles based on the results of the collision risk assessment. Therefore, when crossing the starboard side of an activated obstacle, the USV turns toward the starboard to pass through the obstacle on its port side, as shown in Fig. 10(c).
4) Although COLREGS 13 allows overtaking on the port or starboard side of the USV, the convention on water requires that the overtaking USV should pass obstacles on its port side. Therefore, when an obstacle is overtaken, the USV turns on the starboard to pass the obstacle on its port side, as shown in Fig. 10(d).
5) According to COLREGS 13 and 17, when overtaken by an obstacle, the USV should stand on or turn toward the starboard or port to pass the obstacle. Combining the former two assumptions and considering that the CA strategy requires symmetry to guarantee the matching role of the USV and obstacle, the USV turns to the port to pass the obstacle on its starboard side when overtaken by an obstacle, as shown in Fig. 10(e).

Consequently, for a single activated obstacle O_i approaching the USV
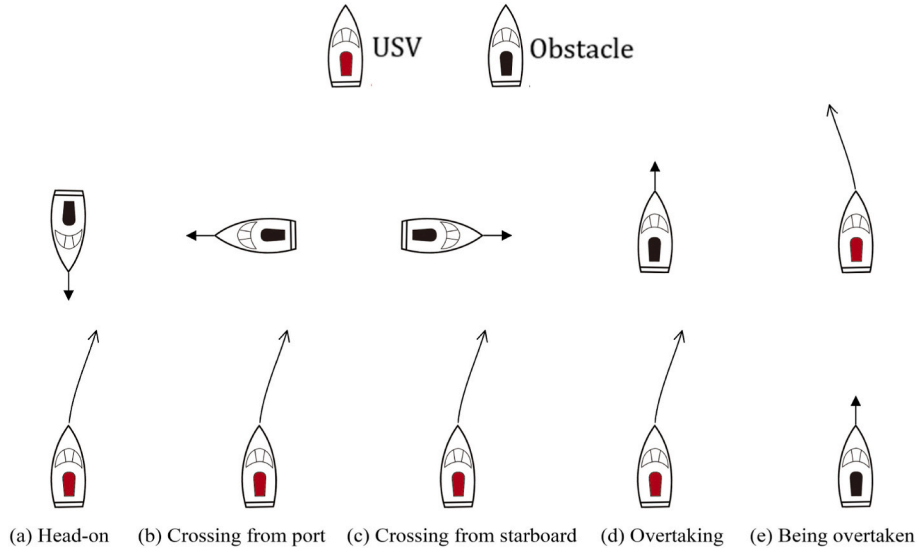
Fig. 10. Assumptions based on COLREGS 13–17: the red and black ships represent USVs and obstacles, respectively.

from any direction, the USV avoids it from the right side of $\overrightarrow{v}_d^{Oi}$. However, for multiple obstacles simultaneously approaching the USV, the USV may not be able to satisfy COLREGS. In this case, the USV preferentially avoids one of the obstacles. Subsequently, the above assumptions were applied to the proposed equivalent obstacle method.

3.3.1. CA strategy based on equivalent obstacle method

The CA velocity, which is designed based on the proposed equivalent obstacle method, can be expressed as $\overrightarrow{v}_{dO}$.

$$\overrightarrow{v}_{dO} = \overrightarrow{v}_d + \overrightarrow{v}_{OD} \tag{48}$$

where $\overrightarrow{v}_{OD}$ is the offset velocity parallel to the straight line l_{OD}, and $\overrightarrow{v}_{OD}$ is designed based on three different encounter situations.

1) Encounter situation $S = 1$.

The USV passes all the forward obstacles on its port side. To reduce the deviation from the desired trajectory during CA, the offset velocity was designed as

$$\overrightarrow{v}_{OD} = \begin{cases} 0 \cdot \overrightarrow{OD}, & EO_{max}^f \le 0 \\ EO_{max}^f \cdot \overrightarrow{OD}, & others \end{cases} \tag{49}$$

2) Encounter situation $S = -1$.

The USV passes all the rear obstacles on its starboard side. To reduce the deviation from the desired trajectory during CA, the offset velocity was designed as

$$\overrightarrow{v}_{OD} = \begin{cases} 0 \cdot \overrightarrow{OD}, & EO_{min}^r \ge 0 \\ EO_{min}^r \cdot \overrightarrow{OD}, & others \end{cases} . \tag{50}$$

3) Encounter situation $S = 0$.

a) When $EO_{max}^f > EO_{min}^r$, USV cannot simultaneously satisfy the COLREGS with each activated obstacle, as shown in Fig. 11 (a). The USV prioritizes turning toward the starboard to pass all the activated obstacles on its port side. The offset velocity is designed as
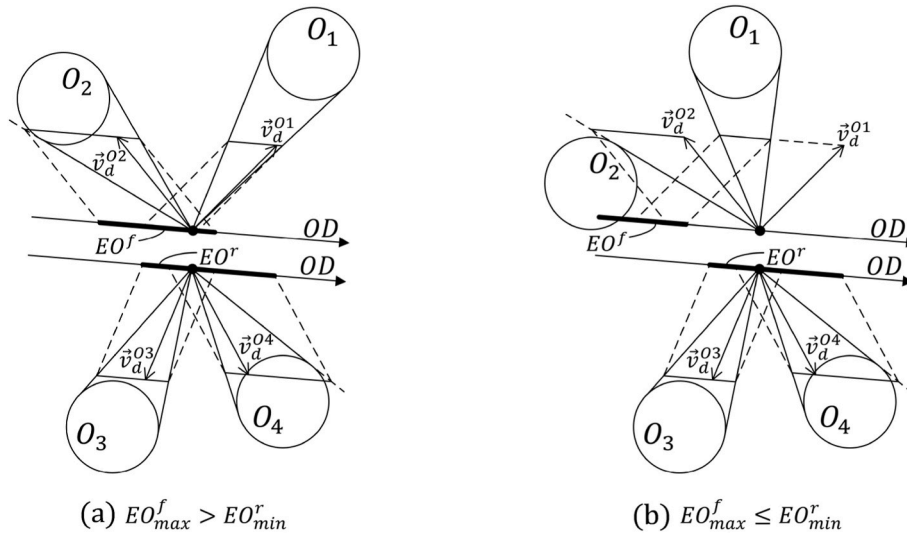

Fig. 11. Encounter situation $S = 0$: USV must avoid the forward equivalent obstacle EO^f and rear equivalent obstacle EO^r. For presentation purposes, EO^f and EO^r are shown in the same parse chart.

$$\vec{v}_{OD} = \begin{cases} 0 \cdot \overrightarrow{OD}, & \max \left(EO^f \cup EO^r \right) \leq 0 \\ \max \left(EO^f \cup EO^r \right) \cdot \overrightarrow{OD}, & others \end{cases}. \quad (51)$$

b) When $EO^f_{max} \leq EO^r_{min}$, the USV passes all the forward obstacles on its port side and all the rear obstacles on its starboard side, as shown in Fig. 11(b). To reduce the deviation from the desired trajectory during CA, the offset velocity was designed as

$$\vec{v}_{OD} = \begin{cases} 0 \cdot \overrightarrow{OD} & EO^f_{max} \leq 0 \leq EO^r_{min} \\ EO^f_{max} \cdot \overrightarrow{OD} & EO^f_{max} > 0 \\ EO^r_{min} \cdot \overrightarrow{OD} & others \end{cases}. \quad (52)$$

3.3.2. CA strategy in emergency situations

Although the USV can avoid obstacles by tracking the designed CA velocity $\vec{v}_{dO}$, it may enter hazardous obstacle areas because of disturbances in the marine environment and the self-motion control errors of the USVs. To further ensure that a safe distance can be maintained between the USV and obstacles, an emergency CA module was added. In situations in which the USV is about to enter a hazardous area of an obstacle or is already in the hazardous area, the COLREGS-compliant emergency CA velocity was designed based on the actual velocity of the USV relative to the obstacle. Because this emergency CA module complements the above CA strategy, the emergency CA velocity was designed by considering only one activated obstacle.

To be consistent with the above CA strategy, the USV avoids O_i from the left side of $\vec{v}^{Oi}$ when (53) is satisfied. Otherwise, the USV avoids O_i from the right side of $\vec{v}^{Oi}$. $\vec{v}^{Oi}$ denotes the actual relative velocity of USV relative to O_i.

$$\begin{cases} S = 0 \\ EO^f_{max} > EO^r_{min} \\ D_{Oi} = -1 \end{cases} \quad (53)$$

VO_{Oi} represents the obstacle velocity of O_i in the velocity space of the USV relative to O_i. d_{Oi} and d_s denote the actual and safe distances between the USV and O_i boundaries, respectively. d_{Oi} is expressed as

$$d_{Oi} = \left\| \overrightarrow{p}_{Oi} - \overrightarrow{p} \right\| - R_{Oi} + d_s \quad (54)$$

where R_{Oi} is the distance from $\overrightarrow{p}_{Oi}$ along $\overrightarrow{p} - \overrightarrow{p}_{Oi}$ to the boundary of the expanded O_i. Changing the relative course of a USV is typically the most effective way to avoid collisions in an emergency. $\vec{v}^{Oi}_{eOi}$ denotes the emergency CA velocity of the USV relative to obstacle O_i.

1) When the following conditions are satisfied, the USV is considered to nearly enter the hazardous area of O_i.

$$\begin{cases} d_{Oi} \geq d_s \\ \vec{v}^{Oi} \in VO_{Oi} \\ t_{aOi} \leq t_e \end{cases} \quad (55)$$

where $t_{aOi} = \left\| \overrightarrow{p}^{Oi} \right\| / \left\| \vec{v}^{Oi} \right\|$ is the time to collision of the USV with the expanded O_i, as shown in (8). $\overrightarrow{p}^{Oi}$ denotes the position vector from the

current position of the USV along the velocity $\vec{v}^{Oi}$ to the boundary of the expanded O_i. Threshold $t_e < t_r$ is used to determine whether the USV is about to enter a hazardous area of O_i.

a) If (53) is not satisfied, then the USV avoids O_i from the right side of $\vec{v}^{Oi}$. $\vec{v}^{Oi}_{eOi}$ was selected by rotating $\vec{v}^{Oi}$ to the right, parallel to $\overrightarrow{p}^{Oi}_R$, as shown in Fig. 12(a). Therefore, $\vec{v}^{Oi}_{eOi}$ can be obtained using the following conditions:

$$\begin{cases} \vec{v}^{Oi}_{eOi} \parallel \overrightarrow{p}^{Oi}_R \\ \left\| \vec{v}^{Oi}_{eOi} \right\| = \left\| \vec{v}^{Oi} \right\| \\ \vec{v}^{Oi}_{eOi} \cdot \overrightarrow{p}^{Oi}_R > 0 \end{cases} \quad (56)$$

b) If (53) is satisfied, then the USV avoids O_i from the left side of $\vec{v}^{Oi}$. $\vec{v}^{Oi}_{eOi}$ was selected by rotating $\vec{v}^{Oi}$ to the left, parallel to $\overrightarrow{p}^{Oi}_L$, as shown in Fig. 12(b). Therefore, $\vec{v}^{Oi}_{eOi}$ can be obtained using the following conditions:

$$\begin{cases} \vec{v}^{Oi}_{eOi} \parallel \overrightarrow{p}^{Oi}_L \\ \left\| \vec{v}^{Oi}_{eOi} \right\| = \left\| \vec{v}^{Oi} \right\| \\ \vec{v}^{Oi}_{eOi} \cdot \overrightarrow{p}^{Oi}_L > 0 \end{cases} \quad (57)$$

2) When the following conditions are satisfied, the USV is considered to be already in a hazardous area of O_i.

$$\begin{cases} d_{Oi} < d_s \\ \vec{v}^{Oi} \cdot \left(\overrightarrow{p}_{Oi} - \overrightarrow{p} \right) > 0 \end{cases} \quad (58)$$

a) If (53) is not satisfied, then the USV avoids O_i from the right side of $\vec{v}^{Oi}$. $\vec{v}^{Oi}_{eOi}$ was selected by rotating $\vec{v}^{Oi}$ to the right, perpendicular to $(\overrightarrow{p}_{Oi} - \overrightarrow{p})$, as shown in Fig. 13(a). Therefore, $\vec{v}^{Oi}_{eOi}$ can be obtained using the following conditions:

$$\begin{cases} \vec{v}^{Oi}_{eOi} \perp \left(\overrightarrow{p}_{Oi} - \overrightarrow{p} \right) \\ \left\| \vec{v}^{Oi}_{eOi} \right\| = \left\| \vec{v}^{Oi} \right\| \\ \left(\angle \vec{v}^{Oi}_{eOi} - \angle \left(\overrightarrow{p}_{Oi} - \overrightarrow{p} \right) \right) \backslash 2\pi < \pi \end{cases} \quad (59)$$

b) If (53) is satisfied, then the USV avoids O_i from the left side of $\vec{v}^{Oi}$. $\vec{v}^{Oi}_{eOi}$ was selected by rotating $\vec{v}^{Oi}$ to the left, perpendicular to $(\overrightarrow{p}_{Oi} - \overrightarrow{p})$, as shown in Fig. 13(b). Therefore, $\vec{v}^{Oi}_{eOi}$ can be obtained using the following conditions:

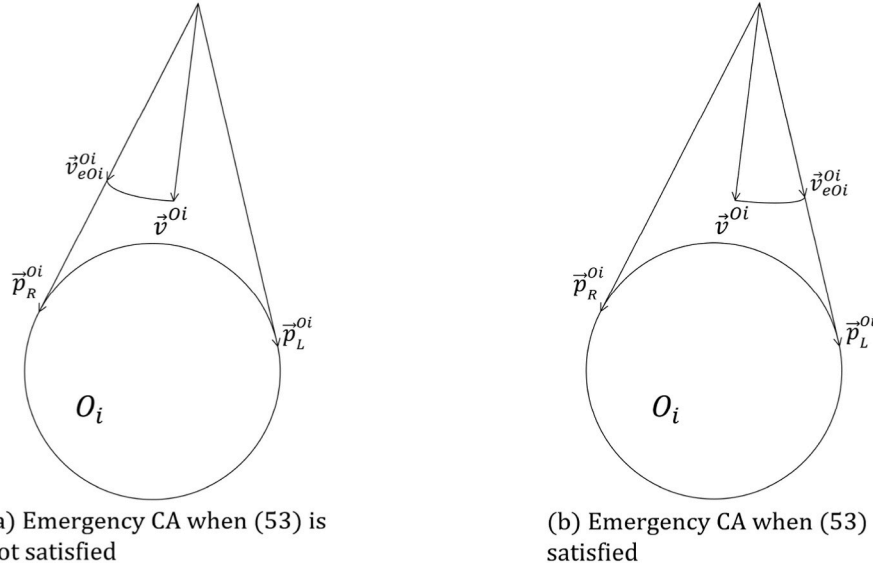(a) Emergency CA when (53) is not satisfied

(b) Emergency CA when (53) is satisfied

Fig. 12. Emergency CA: USV is about to enter the hazardous area of O_i. The circle represents the expanded obstacle.

(a) Emergency CA when (53) is not satisfied

(b) Emergency CA when (53) is satisfied

Fig. 13. Emergency CA: USV is already in the hazardous area of O_i. The circle represents the expanded obstacle.

$$
\begin{cases}
\overrightarrow{v}^{Oi}_{eOi} \perp \left(\overrightarrow{p}_{Oi} - \overrightarrow{p} \right) \\
\left\| \overrightarrow{v}^{Oi}_{eOi} \right\| = \left\| \overrightarrow{v}^{Oi} \right\| \\
\left(\angle \overrightarrow{v}^{Oi}_{eOi} - \angle \left(\overrightarrow{p}_{Oi} - \overrightarrow{p} \right) \right) \big\backslash 2\pi > \pi
\end{cases}
\tag{60}
$$

Therefore, for each activated obstacle, the emergency CA velocity designed based on the proposed CA strategy can be expressed as $\overrightarrow{v}_{eOi}$.

$$
\overrightarrow{v}_{eOi} = \begin{cases}
\overrightarrow{v} + \overrightarrow{v}^{Oi}_{eOi} - \overrightarrow{v}^{Oi}, & (55) \ or \ (58) \text{is satisfied} \\
\overrightarrow{v}, & others
\end{cases}
\tag{61}
$$

Furthermore, when there are multiple activated obstacles that require emergency CA, the USV should prioritize avoiding obstacles

with the highest collision risk. Therefore, the following cost function was established:

$$
J_e\left(\overrightarrow{v}_{eOi} \right) = \begin{cases}
d_{Oi}, & (58) \text{is satisfied} \\
d_s + t_{aOi}, & (55) \text{is satisfied} \\
+\infty, & others
\end{cases}
\tag{62}
$$

For all activated obstacles, the emergency CA velocity is designed as

$$
\overrightarrow{v}_{eO} = \underset{\overrightarrow{v}_{eOi}}{\arg\min} J_e\left(\overrightarrow{v}_{eOi} \right)
\tag{63}
$$

In summary, the CA velocity designed based on the proposed CA strategy can be expressed as follows:

$$\vec{v}_c = \begin{cases} \vec{v}_{eO}, & \min J_e\left(\vec{v}_{eOi}\right) \neq +\infty \\ \vec{v}_{dO}, & others \end{cases}. \tag{64}$$

When n obstacles are activated, the design process of $\vec{v}_c$ is implemented as shown in Algorithm 2.

Algorithm 2. Design Collision Avoidance Velocity

Algorithm 2 Design Collision Avoidance Velocity
Input: t_e, d_s, $\vec{v}_d$, $\vec{v}$, $\vec{p}$, $\vec{v}_{Oi}$, $\vec{p}_{Oi}$, VO_{Oi}, where $i = 1, 2, \ldots, n$
Output: $\vec{v}_c$
Procedure:
1: compute l_{OD} according to (17)-(20)
2: compute $\overrightarrow{OD}$
3: **for** $i = 1$ to n **do**
4:     determine D_{Oi} according to (21)-(22)
5:     compute OD^{Oi} according to (23)-(31) and (34)-(39)
6:     compute OD^{fOi} and OD^{rOi} according to (43)-(44)
7:     compute d_{Oi} according to (54)
8:     **if** $d_{Oi} \geq d_s$ **then**
9:         compute $\vec{v}_{eOi}^{Oi}$ according to (53) and (55)-(57)
10:     **else**
11:         compute $\vec{v}_{eOi}^{Oi}$ according to (53) and (58)-(60)
12:     **end if**
13:     compute $\vec{v}_{eOi}$ and $J_e(\vec{v}_{eOi})$ according to (61)-(62)
14: **end for**
15: compute $\vec{v}_{eO}$ according to (63)
16: **if** $\min J_e(\vec{v}_{eOi}) \neq +\infty$ **then**
17:     $\vec{v}_c \leftarrow \vec{v}_{eO}$
18: **else**
19:     compute EO^f and EO^r according to (40)-(42)
20:     determine encounter situation S
21:     **if** $S = 1$ **then**
22:         compute $\vec{v}_{OD}$ according to (49)
23:     **else if** $S = -1$ **then**
24:         compute $\vec{v}_{OD}$ according to (50)
25:     **else**
26:         compute $\vec{v}_{OD}$ according to (51)-(52)
17:     **end if**
18:     compute $\vec{v}_{dO}$ according to (48)
29:     $\vec{v}_c \leftarrow \vec{v}_{dO}$
30: **end if**

4. Simulation results

In this section, the simulation results for several typical multiship encounters are presented. Throughout the simulations, it was assumed that each USV considered the other USVs as obstacles. The update fre-quency of the motion information of the USV and obstacles was 10 Hz (i. e., $t_\Delta = 0.1$). The algorithm was implemented using Python and run in an existing simulator using a laptop with an Intel (R) Core (TM) i5-9300H 2.40 GHz processor and 8 GB RAM. The simulator was developed using Unity, which is a 3D engine tool. The data between the simulator and the proposed algorithm were transmitted in the form of messages via network communication.

We used the same USV model with the dimensions of 9×4 (length $\times$ width) and 3000 mass, as shown in Fig. 14(a). In the algorithm, the shape of the USV was simplified to a circle with a radius of 5 m, as shown in Fig. 14(b). The safe distance was set to $d_s = 4$. The kinematic constraints of the USVs when avoiding collisions were designed as $[W_{min}, W_{max}, a_{Vmin}, a_{Vmax}] = [-0.2, 0.2, -1, 1]$. A rectangular coordinate system was established with 123° east longitude, 28° north latitude as the origin, and the X axis pointing to the north. The basic parameters for the trajectory-planning set for the seven USVs are listed in Table 1tbl1, including the start position $\vec{p}_s$, target position $\vec{p}_t$, desired approach speed U_d, and initial heading angle H_0.

4.1. Encounter situation $S = 1$

The simulations included USV0, USV3, USV4, and USV6. As shown in Fig. 15(a), the USVs initially approach their target positions directly. When at least one activated obstacle is detected through the collision risk assessment described in Section 2.2, the USVs change course and perform the CA maneuver conforming to COLREGS according to Algorithm 2. After no activated obstacles exist, the USVs' velocities gradually restored to their desired velocities under the kinematic constraints described in Section 2.3. Subsequently, the USVs continue to approach their respective target positions directly. According to the equivalent obstacle method proposed in Section 3.2, USV3, USV4, and USV6 can be considered as forward obstacles for USV0. The screenshots of the CA

Table 1
Basic parameters for trajectory planning set for the seven USVs.

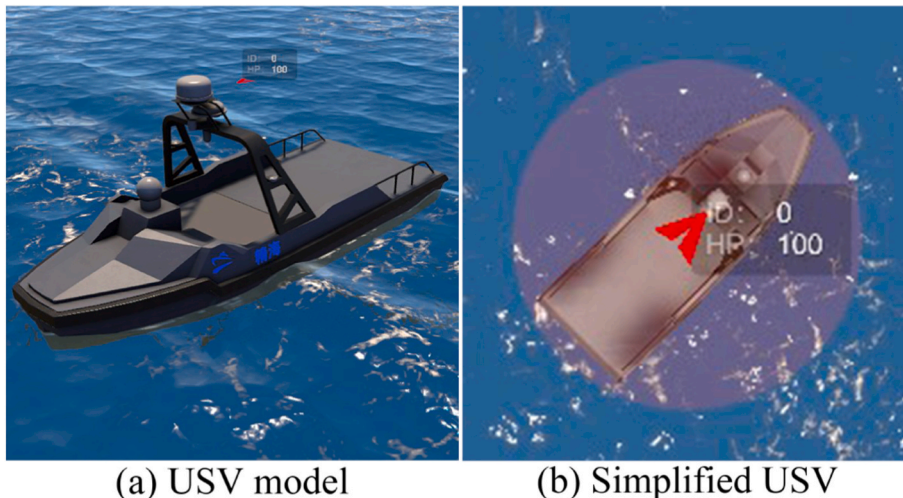| Name	$\vec{p}_s$	$\vec{p}_t$	U_d	H_0
USV0	(-78, −78)	(162, 162)	$4\sqrt{2}$	0.25π
USV1	(81, −238)	(81, 242)	8	0.5π
USV2	(-238, 83)	(242, 83)	8	0
USV3	(241, −79)	(1, 161)	$4\sqrt{2}$	0.75π
USV4	(-77, 243)	(163, 3)	$4\sqrt{2}$	1.75π
USV5	(-239, −237)	(241,243)	$8\sqrt{2}$	0.25π
USV6	(243, 241)	(3, 1)	$4\sqrt{2}$	1.25π

(a) USV model   (b) Simplified USV

Fig. 14. USV model used in the simulator. In the proposed CA approach, the shape of USV is simplified to a circle.
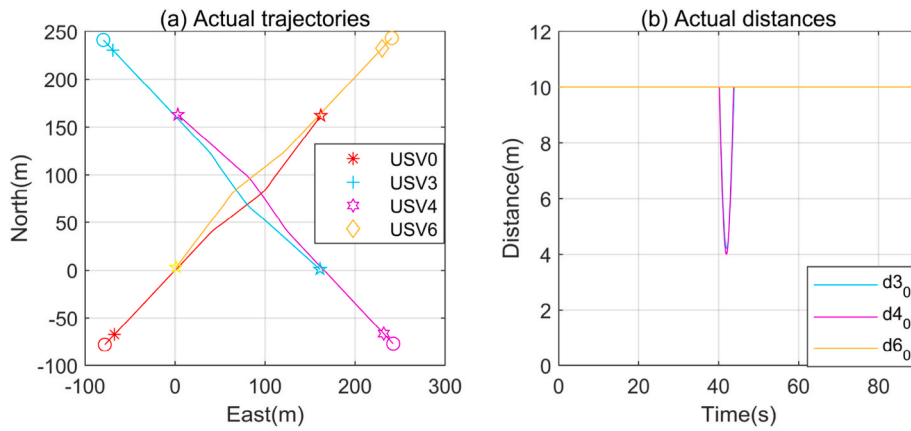
Fig. 15. Actual trajectories of all USVs and actual distances between USV0 and each obstacle: start positions are marked by ◯. Target positions are marked by ☆. d_{ij} denotes the actual distance between USV i boundary and USV j boundary. The upper limit of d_{ij} is set to 10 for the convenience of showing the results.
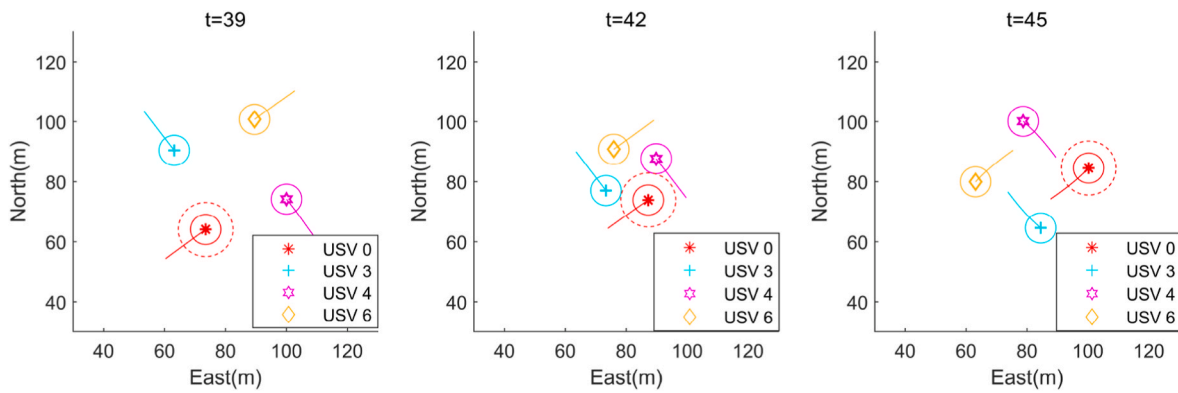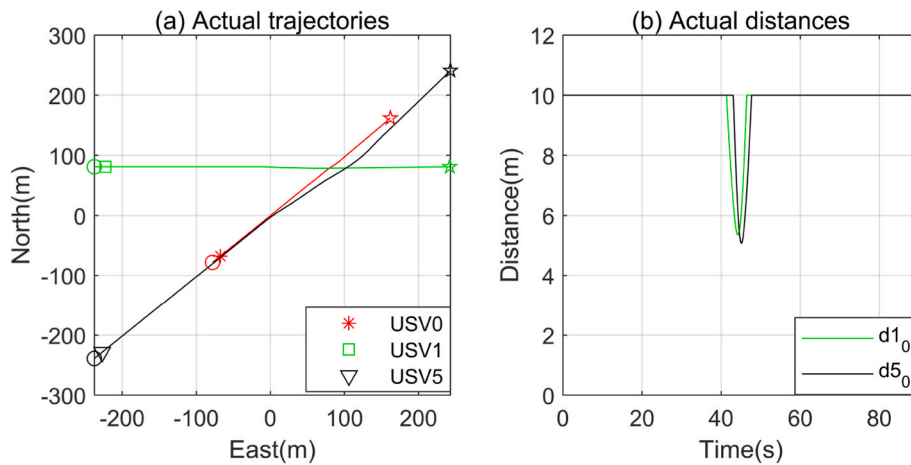

Fig. 16. Screenshots of collision avoidance process: the solid line segments represent the trajectories that the USVs have traveled in the past 3 seconds. The solid line circles represent simplified USVs. The radius of the dashed circle is equal to the radius of the simplified USV 0 in addition to the safety distance.

Fig. 17. Actual trajectories of all USVs and actual distances between USV0 and each obstacle: start positions are marked by ◯. Target positions are marked by ☆. d_{ij} denotes the actual distance between USV i boundary and USV j boundary. The upper limit of d_{ij} is set to 10 for the convenience of showing the results.

process in Fig. 16 show that USV0 turns toward the starboard to pass all obstacles on its port side according to the CA strategy proposed in Section 3.3. USV0 maintains a safe distance from the obstacles during the entire movement, as shown in Fig. 15(b).

4.2. Encounter situation $S = -1$

The simulations included USV0, USV1, and USV5. As shown in Fig. 17(a), the USVs initially approach their respective target positions directly. When at least one activated obstacle is detected through the collision risk assessment described in Section 2.2, the USVs change course and perform the CA maneuver conforming to COLREGS
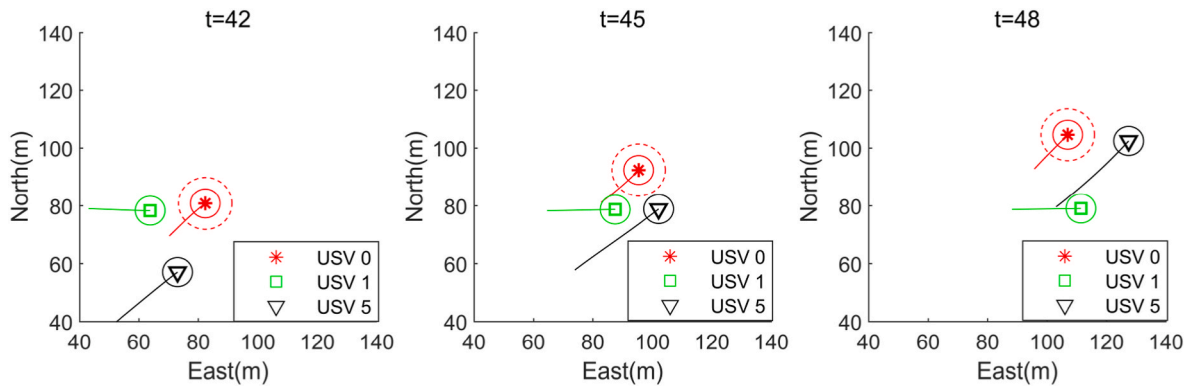
Fig. 18. Screenshots of collision avoidance process: the solid line segments represent trajectories that the USVs have traveled in the past 3 seconds. The solid line circles represent simplified USVs. The radius of the dashed circle is equal to the radius of the simplified USV0 in addition to the safety distance.

according to Algorithm 2. After no activated obstacles exist, the USVs' velocities gradually restored to their desired velocities under the kinematic constraints described in Section 2.3. Subsequently, the USVs continue to approach their respective target positions directly. According to the equivalent obstacle method proposed in Section 3.2, USV1 and USV5 can be considered as rear obstacles for USV0. The screenshots of the CA process in Fig. 18 show that USV0 turns to the port to pass all obstacles on its starboard side, according to the CA strategy proposed in Section 3.3. USV0 maintains a safe distance from the obstacles during the entire movement, as shown in Fig. 17(b)

4.3. Encounter situation $S = 0$

4.3.1. Being sandwiched

In this section, we consider the situation in which USV0 is sandwiched between USV5 and USV6 from the bow and stern, respectively. According to the assumptions in Fig. 10, USV0 should turn to the port to pass USV5 on its starboard side and simultaneously turn toward the starboard to pass USV6 on its port side. The conflicting responsibilities of USV0 can be resolved using the CA strategy proposed in Section 3.3.1 (**Encounter situation $S = 0$**). If USV5 or USV6 does not comply with COLREGS, the following four cases are analyzed:

1) The simulation results when neither USV5 nor USV6 complies with COLREGS are shown in Fig. 19. As shown in Fig. 19(a), USV0 initially approaches the target positions directly. When at least one activated obstacle is detected through the collision risk assessment described

in Section 2.2, the USV0 changes course and performs the CA maneuver conforming to COLREGS according to Algorithm 2. After no activated obstacles exist, the USV0 velocity gradually restored to the desired velocity under the kinematic constraints described in Section 2.3. Subsequently, the USV0 continues to approach the target position directly. USV0 turns toward the starboard to pass all the obstacles on its port side according to the CA strategy proposed in Section 3.3. USV0 maintains a safe distance from the obstacles during the entire movement, as shown in Fig. 19(b)

2) The simulation results when USV5 does not comply with COLREGS are shown in Fig. 20. As in Case 1, according to the CA strategy proposed in Section 3.3, USV0 turns toward the starboard to pass USV5 on its port side. USV0 maintains a safe distance from the obstacles during the entire movement, as shown in Fig. 20(b).

3) The simulation results when USV6 does not comply with COLREGS are shown in Fig. 21. As shown in Fig. 21(a), USV0 performs the CA maneuver conforming to COLREGS after encountering obstacles, and finally reaches the target positions. USV0 turns toward the starboard to avoid all obstacles according to the CA strategy proposed in Section 3.3. Similarly, USV5 turns into a starboard. After USV5 makes sufficient avoidance maneuvers ($EO_{max}^f \leq 0 \leq EO_{min}^r$), there is no need for USV0 to continue turning toward the starboard. Therefore, USV0 continues to move toward the target position at the desired speed. USV0 maintains a safe distance from the obstacles during the entire movement, as shown in Fig. 21(b).

4) The simulation results when both USV5 and USV6 comply with COLREGS are shown in Fig. 22. Similar to Case 3, according to the
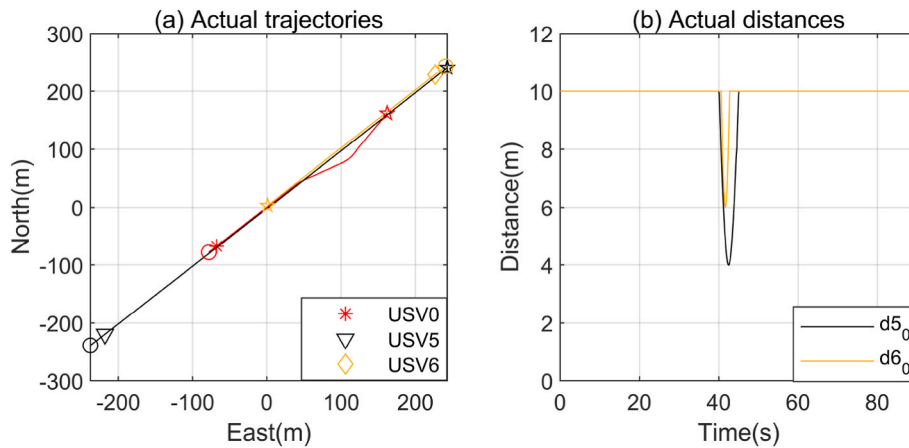

Fig. 19. The case of both USV5 and USV6 do not comply with COLREGS: (a) actual trajectories of all USVs. (b) actual distances between USV0 and each obstacle. Start positions are marked by ◯. Target positions are marked by ☆. d_{ij} denotes the actual distance between USV i boundary and USV j boundary. The upper limit of d_{ij} is set to 10 for the convenience of showing the results.
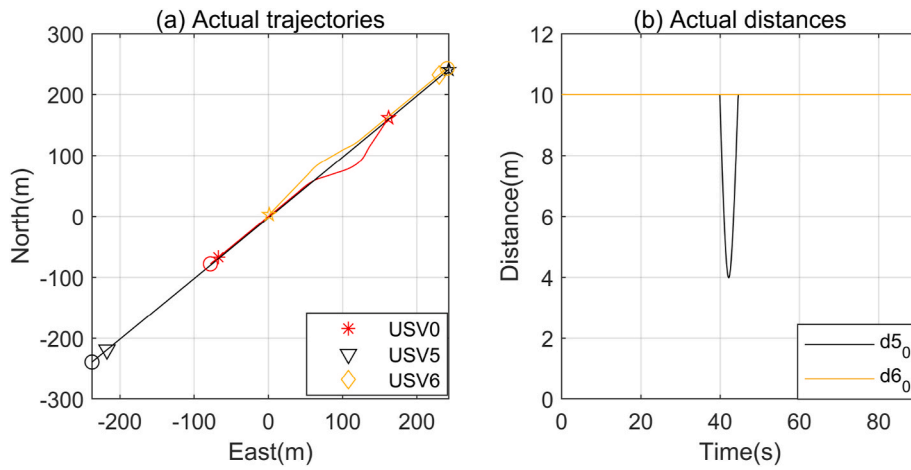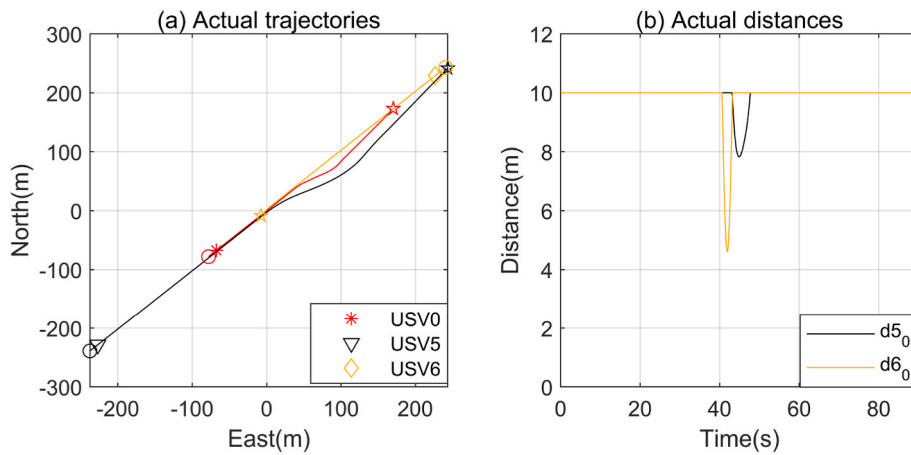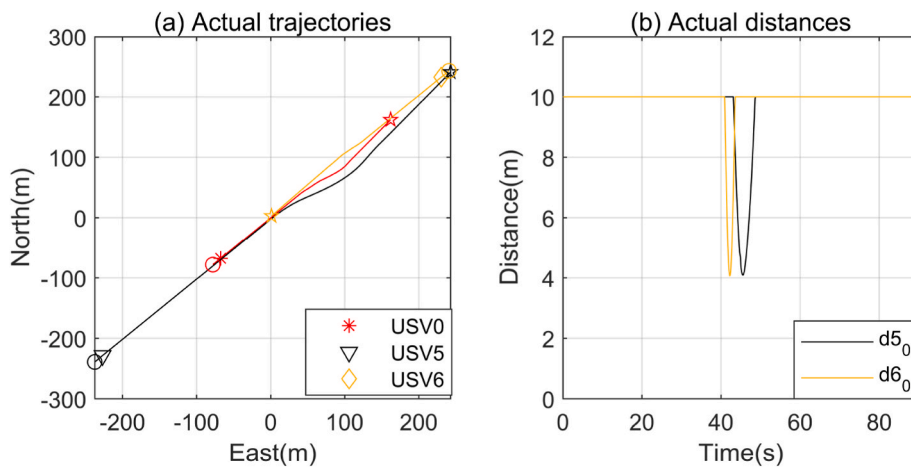
Fig. 20. The case of USV5 does not comply with COLREGS: (a) actual trajectories of all USVs. (b) actual distances between USV0 and each obstacle. Start positions are marked by ◯. Target positions are marked by ☆. d_{ij} denotes the actual distance between USV i boundary and USV j boundary. The upper limit of d_{ij} is set to 10 for the convenience of showing the results.

Fig. 21. The case of USV6 does not comply with COLREGS: (a) actual trajectories of all USVs. (b) actual distances between USV0 and each obstacle. Start positions are marked by ◯. Target positions are marked by ☆. d_{ij} denotes the actual distance between USV i boundary and USV j boundary. The upper limit of d_{ij} is set to 10 for the convenience of showing the results.

Fig. 22. The case of both USV5 and USV6 comply with COLREGS: (a) actual trajectories of all USVs. (b) actual distances between USV0 and each obstacle. Start positions are marked by ◯. Target positions are marked by ☆. d_{ij} denotes the actual distance between USV i boundary and USV j boundary. The upper limit of d_{ij} is set to 10 for the convenience of showing the results.
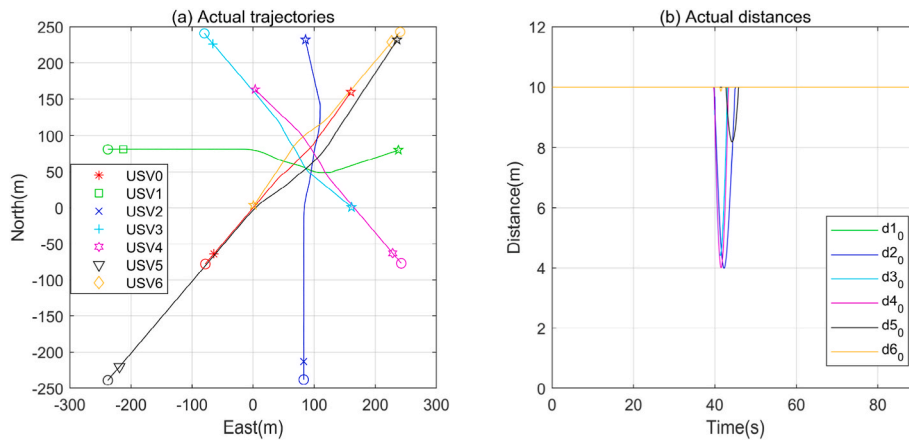
Fig. 23. Actual trajectories of all USVs and actual distances between USV0 and each obstacle: start positions are marked by ◯. Target positions are marked by ☆. d_{ij} denotes the actual distance between USV i boundary and USV j boundary. The upper limit of d_{ij} is set to 10 for the convenience of showing the results.

proposed CA strategy in Section 3.3, USV0 does not continue to turn toward the starboard to avoid all obstacles. After USV5 and USV6 make sufficient avoidance maneuvers ($EO_{max}^f \le 0 \le EO_{min}^r$), USV0 continues to move toward the target position. USV0 maintains a safe distance from the obstacles during the entire movement, as shown in Fig. 22(b).

4.3.2. Being surrounded

In this section, we consider the situation in which USV0 is surrounded and approached by six USVs from all sides. As shown in Fig. 23 (a), the USVs initially approach their target positions. When at least one activated obstacle is detected through the collision risk assessment described in Section 2.2, the USVs change course and perform the CA maneuver conforming to COLREGS according to Algorithm 2. After no

activated obstacles exist, the USVs' velocities gradually restored to their desired velocities under the kinematic constraints described in Section 2.3. Subsequently, the USVs continue to approach their respective target positions directly. According to the equivalent obstacle method proposed in Section 3.2, the other USVs can be considered as two equivalent obstacles for USV0. The screenshots of the CA process in Fig. 24 show that USV0 turns toward the starboard to avoid all obstacles according to the CA strategy proposed in Section 3.3. After other USVs perform sufficient avoidance maneuvers, USV0 continues to move toward the target position. USV0 maintains a safe distance from the obstacles during the entire movement, as shown in Fig. 23(b). In addition, the other USVs maintain a safe distance from the obstacles they detected, as shown in Fig. 25.

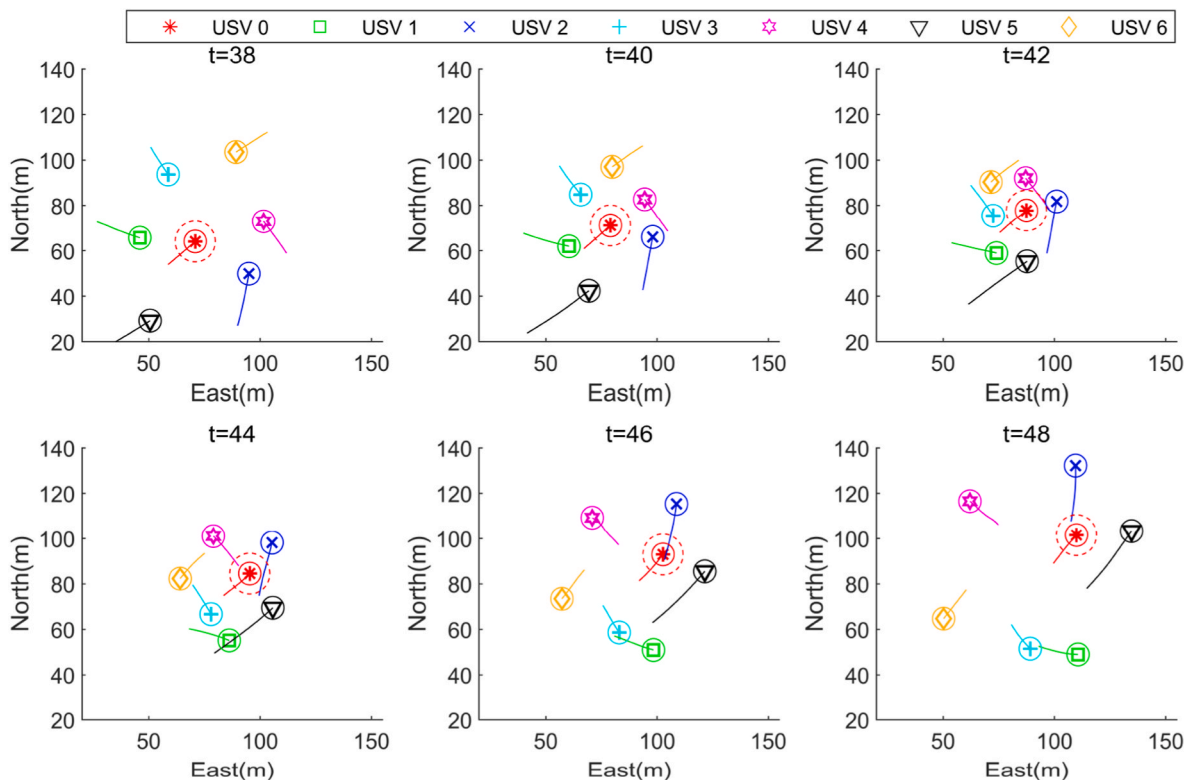To summarize, the simulation results from Section 4.1 and Section

Fig. 24. Screenshots of collision avoidance process: the solid line segments represent trajectories that the USVs have traveled in the past 3 seconds. The solid line circles represent simplified USVs. The radius of the dashed circle is equal to the radius of the simplified USV in addition to the safety distance.
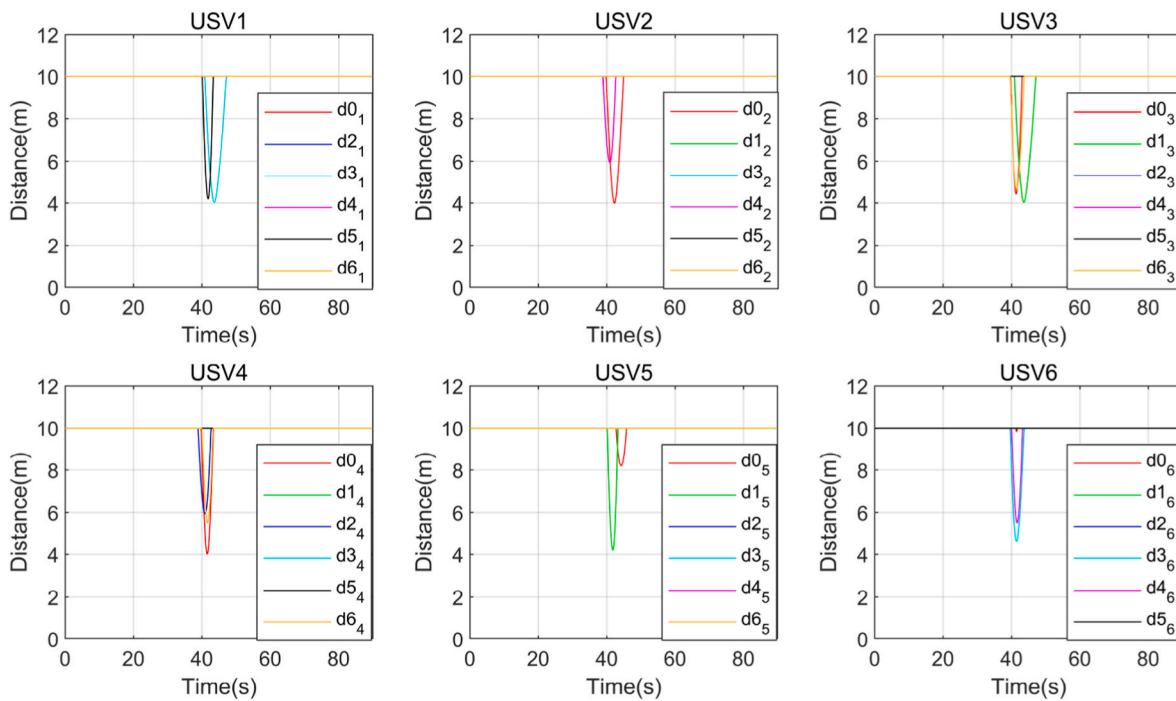
Fig. 25. Actual distances between other USVs and obstacles they detect. di_j denotes the actual distance between USV i boundary and USV j boundary. The upper limit of di_j is set to 10 for the convenience of showing the results.

4.2 demonstrate the effectiveness of the proposed equivalent obstacle method. The simulation results from Section 4.3.1 show that the proposed collision avoidance strategy remains effective when other USVs do not comply by the COLREGS. In addition, the robustness of the proposed trajectory planning approach was verified by an example of the simultaneous collision avoidance of multiple USVs (Section 4.3.2).

5. Conclusion, limitations, and future work

This study addresses the trajectory planning problem of USVs in multiship encounters. In the proposed trajectory planning approach, the equivalent obstacle concept is innovatively presented to simplify the analysis of encounter situations. A COLREGS-compliant CA strategy was presented based on the proposed equivalent obstacle method. The strategy includes an emergency CA module to ensure that a safe distance is maintained between the USV and traffic ships. The performance of the proposed trajectory planning approach was verified through physical simulations using an existing simulator. Furthermore, the approach remains effective when other ships ignore their responsibilities under COLREGS.

The trajectory planning algorithm proposed in this study does not consider the packet loss of sensor data or impaired maneuverability of the USV. Packet loss of sensor data can affect the maintenance of a safe distance between the USV and obstacles to a certain extent. A USV with impaired maneuverability may collide with obstacles because of its inability to track a planned CA trajectory efficiently.

In future work, we plan to develop collision-free trajectories for USVs with impaired maneuverability in the presence of packet loss from sensor data. Additionally, different ocean topographies will be considered.

CRediT authorship contribution statement

Jianjian Liu: Conceptualization, Investigation, Software, Validation, Writing – original draft. **Huizi Chen:** Methodology, Writing – review & editing. **Shaorong Xie:** Investigation, Methodology. **Yan Peng:** Methodology, Writing – review & editing. **Dan Zhang:** Project administration, Supervision, Writing – review & editing. **Huayan Pu:** Investigation, Methodology.

Declaration of competing interest

The authors declare that they have no known competing financial interests or personal relationships that could have appeared to influence the work reported in this paper.

Data availability

The data that has been used is confidential.

References

Blaich, M., Köhler, S., Reuter, J., Hahn, A., 2015. Probabilistic collision avoidance for vessels. IFAC-PapersOnLine 48 (16), 69–74.

Breivik, M., 2010. Topics in Guided Motion Control of Marine Vehicles.

Candeloro, M., Lekkas, A.M., Sørensen, A.J., Fossen, T.I., 2013. Continuous curvature path planning using voronoi diagrams and fermat's spirals. IFAC Proc. Vol. 46 (33), 132–137.

Cheng, Y., Zhang, W., 2018. Concise deep reinforcement learning obstacle avoidance for underactuated unmanned marine vessels. Neurocomputing 272, 63–73.

Cho, Y., Han, J., Kim, J., 2020. Efficient COLREG-compliant collision avoidance in multi-ship encounter situations. IEEE Trans. Intell. Transport. Syst. 23 (3), 1899–1911.

Fiorini, P., Shiller, Z., 1998. Motion planning in dynamic environments using velocity obstacles. Int. J. Robot. Res. 17 (7), 760–772.

Hwang, C.N., Yang, J.M., Chiang, C.Y., 2001. The design of fuzzy collision-avoidance expert system implemented by H∞-autopilot. J. Mar. Sci. Technol. 9 (1), 4.

Huang, Y., Chen, L., van Gelder, P.H.A.J.M., 2019. Generalized velocity obstacle algorithm for preventing ship collisions at sea. Ocean Eng. 173, 142–156.

International Maritime Organization, 1972. Convention on the International Regulations for Preventing Collisions at Sea, 1972 (COLREGs).

Junmin, M., Mengxia, L., Weixuan, H., 2021. Mechanism of dynamic automatic collision avoidance and the optimal route in multi-ship encounter situations. J. Mar. Sci. Technol. 26, 141–158.

Kluge, B., Prassler, E., 2004. Reflective navigation: individual behaviors and group behaviors. In: IEEE International Conference on Robotics and Automation, 2004. Proceedings. ICRA'04. 2004, vol. 4. IEEE, pp. 4172–4177.

Kufoalor, D.K.M., Brekke, E.F., Johansen, T.A., 2018. Proactive collision avoidance for ASVs using a dynamic reciprocal velocity obstacles method. In: 2018 IEEE/RSJ International Conference on Intelligent Robots and Systems (IROS). IEEE, pp. 2402–2409.

Kuwata, Y., Wolf, M.T., Zarzhitsky, D., Huntsberger, T.L., 2013. Safe maritime autonomous navigation with COLREGS, using velocity obstacles. IEEE J. Ocean. Eng. 39 (1), 110–119.

LaValle, S.M., 2006. Planning Algorithms. Cambridge university press.

Lyu, H., Yin, Y., 2019. COLREGS-constrained real-time path planning for autonomous ships using modified artificial potential fields. J. Navig. 72 (3), 588–608.

Liu, Y., Song, R., Bucknall, R., 2015. A practical path planning and navigation algorithm for an unmanned surface vehicle using the fast marching algorithm. In: OCEANS 2015-Genova. IEEE, pp. 1–7.

Loe, Ø.A.G., 2008. Collision Avoidance for Unmanned Surface Vehicles. Master's thesis. Institutt for teknisk kybernetikk.

Medyna, P., Mąka, M., 2012. Determination of the shortest path as the basis for examining the most weather favorable routes. Zeszyty Naukowe Akademii Morskiej w Szczecinie 32 (104), 29–33.

Snape, J., Van Den Berg, J., Guy, S.J., Manocha, D., 2011. The hybrid reciprocal velocity obstacle. IEEE Trans. Robot. 27 (4), 696–706.

Sun, T., Liu, C., Xu, S., 2022. COLREGS-complied automatic collision avoidance for the encounter situations of multiple vessels. J. Mar. Sci. Eng. 10 (11), 1688.

Tsou, M.C., Hsueh, C.K., 2010. The study of ship collision avoidance route planning by ant colony algorithm. J. Mar. Sci. Technol. 18 (5), 16.

Van den Berg, J., Lin, M., Manocha, D., 2008. Reciprocal velocity obstacles for real-time multi-agent navigation. In: 2008 IEEE International Conference on Robotics and Automation. IEEE, pp. 1928–1935.

Woerner, K.L., Benjamin, M.R., Novitzky, M., Leonard, J.J., 2016. Collision avoidance road test for COLREGS-constrained autonomous vehicles. In: OCEANS 2016 MTS/IEEE Monterey. IEEE, pp. 1–6.

Wu, P., Xie, S., Luo, J., Qu, D., Li, Q., 2015. The USV Path Planning Based on the Combinatorial Algorithm. Revista Tecnica de la Facultad de Ingenieria Universidad del Zulia.

Yang, R., Xu, J., Wang, X., Zhou, Q., 2019. Parallel trajectory planning for shipborne Autonomous collision avoidance system. Appl. Ocean Res. 91, 101875.

Zhang, J., Zhang, D., Yan, X., Haugen, S., Soares, C.G., 2015. A distributed anti-collision decision support formulation in multi-ship encounter situations under COLREGs. Ocean Eng. 105, 336–348.

Zaccone, R., Martelli, M., 2020. A collision avoidance algorithm for ship guidance applications. Journal of Marine Engineering & Technology 19, 62–75.